ERASMUS MUNDUS MASTER IN
MEMBRANE ENGINEERING
FOR A SUSTAINABLE WORLD
EM3E-4SW

With the support of the
Erasmus+ Programme
of the European Union

Academic Year 2020 – 2021

Modified PEEK mixed-matrix membranes for pervaporation applications

Dissertation for obtaining a Master's degree in Membrane Engineering

Erasmus Mundus Master in Membrane Engineering for a Sustainable World

Mary Loisse GRIMALDO

September 2021

Universidad de Zaragoza

Supervisor: Alberto Figoli
Overseer: Reyes Mallada

www.em3e-4sw.eu
www.itm.cnr.it
www.deltamem.ch

The Erasmus Mundus Master in Membrane Engineering for a Sustainable World (EM3E-4SW) is an education programme financed by the European Commission - Education, Audiovisual and Culture Executive Agency (EACEA), under Project Number-574441-EPP-1-2016-1-FR-EPPKA1-JMD-MOB. It is also supported by the European Membrane Society (EMS), the European Membrane House (EMH), and a large international network of industrial companies, research centers and universities.

ACKNOWLEDGEMENTS

Mr. Luigi Leva, for coordinating with Dr. Figoli about my thesis project in order to make this internship opportunity possible.

Dr. Alberto Figoli, for giving me his full support to finish my thesis, and for guiding me all throughout this project.

Dr. Francesco Galiano, for performing some of the characterization tests of my membranes in CNR-ITM and for guiding me in this project.

Dr. Reyes Mallada, for allowing me to do my internship remotely in Instituto de Nanociencia y Materiales de Aragon (INMA), and for guiding me as I work on the synthesis and characterization of the metal-organic frameworks.

DeltaMem, for inviting me to their laboratory to do the pervaporation tests of my membranes. I would like to give special mention to Dr. Wilfredo Yave for all his help, for being such a good mentor guiding me since the very beginning, and for reviewing this report.

The EM3E-4SW Master team and the European Commission for this scholarship and letting me experience many wonderful things, meet wonderful people from all over the world.

And lastly, my family and friends who always serve as my inspiration and for always giving me their encouragement and support, especially in this pandemic times.

Many thanks to everyone who has been part of this incredible Erasmus Mundus master journey.

Abstract

Dehydration of acetic acid through distillation is rather difficult due to tangent pinch at both ends of the vapor-liquid equilibrium which would require high number of stages and reflux ratios to achieve separation. Pervaporation (PV) is a membrane separation technique where one component of a liquid mixture (feed) selectively permeates through a dense membrane. It is used for separations in which distillation is impossible to use or is not economical. However, the problems faced by membranes used in pervaporation is the tradeoff between permeance and selectivity, and particularly, in acidic conditions, the chemical resistance towards acid. Thus, membrane development is geared towards improving this issue by investigating performance of several membrane materials in acidic mixtures such as acetic acid (HAc) and water.

Several dense mixed-matrix membranes, with PEEK-WC as the matrix and metal-organic frameworks (MOFs) as the nanofillers, were investigated in the dehydration of acetic acid by pervaporation. Three MOFs were used: ZIF-8, HKUST-1, and MIL-101(Cr) in two concentrations: 2.5 wt% and 5 wt% by polymer. Characterizations of the synthesized nanofillers are in good agreement with those reported in literature. Moreover, characterizations of the MMMs showed that they are defect-free, slightly hydrophilic in nature, and have good thermal and mechanical properties. Membrane swelling showed that MZ and MH membranes have lower degrees of swelling than the neat PEEK-WC membrane.

Among the five membrane samples, only two membranes (PEEK-WC and MH-2.5) gave stable permeance values. At high acid concentration (5%), PEEK-WC membrane has a water permeance of 1142 GPU with a selectivity of 7.3 and MH-2.5 improved the water permeance (3176 GPU) while having almost same selectivity (7.7) as the neat PEEK-WC membrane. Increasing further the nanofiller content to 5 wt% (MH-5) loses the selectivity. This showed that with the correct choice of nanofillers and the correct nanofiller loading, MMMs based on PEEK-WC can improve the pervaporation performance of the membrane by increasing its water permeance.

Keywords: pervaporation, mixed-matrix membranes, PEEK-WC, metal-organic frameworks, acetic acid

Resumen

La deshidratación del ácido acético a través de la destilación es difícil porque requiere un alto número de etapas y relaciones de reflujo. La pervaporación (PV) es una técnica de separación de membranas donde un componente de una mezcla líquida penetra selectivamente a través de una membrana densa, esta tecnica se utiliza para separaciones donde la destilación es imposible de emplear o no es económica. El problema a los que se enfrentan las membranas es el balance entre la permeabilidad y la selectividad, particularmente, en condiciones ácidas, asi como tambien la resistencia química frente al ácido. Por lo tanto, el desarrollo de las membranas está orientado a mejorar este balance a través de la investigación del rendimiento de varios materiales en mezclas ácidas, como ácido acético y agua.

Se investigaron varias membranas compósitas (MMM) densas con PEEK-WC como matriz para la deshidratación de ácido acético mediante pervaporación. Se utilizaron tres MOFs: ZIF-8, HKUST-1 y MIL-101(Cr) en dos concentraciones: 2.5 wt% and 5 wt% respecto al polímero. Las caracterizaciones de las nanoparticulas sintetizadas están de acuerdo con los resultados reportados en la literatura. Además, las caracterizaciones de las MMM mostraron que no tienen defectos, son de naturaleza ligeramente hidrofílica y tienen buenas propiedades térmicas y mecánicas. Los tests de hinchamiento mostraron que las membranas MZ y MH tienen grados más bajos de hinchamiento que la membrana PEEK-WC.

De las cinco muestras de membranas, sólo dos (PEEK-WC y MH-2.5) dieron valores estables de permeación. A concentraciones altas de ácido (5%), la membrana PEEK-WC tiene una permeación de agua de 1142 GPU con una selectividad de 7.3 y la membrana MH-2.5 mejoró su permeación (3176 GPU) manteniendo su selectividad (7.7) igual a la de la membrana PEEK-WC. Si el contenido de nanopartículas en la membrana aumenta a 5 wt% (MH-5), la selectividad cae. Esto demostró que con elegir el tipo y el contenido de las nanopartículas apropiadas, las MMM basadas en PEEK-WC pueden mejorar su rendimiento a la permeación del agua.

Keywords: pervaporation, mixed-matrix membranes, PEEK-WC, metal-organic frameworks, acetic acid

Table of Contents

1. Introduction

According to global organic acid production data, acetic acid (HAc; both dilute and glacial) is the most widely industrially used acid particularly for the manufacture of chemicals, being one of the top 20 organic intermediates used in chemical industry[1]. Also, from a report by Expert Market Research, the global acetic acid market reached a volume of 9.07 million tons in 2020 and is forecasted to reach a volume of around 11.85 million tons by 2026[2]. Acetic acid is primarily used as a raw material for the production of vinyl acetate monomer, which is one of its biggest market, and as a reagent for producing compounds such as cellulose acetate, vinyl plastics, latex paints, and textile finishes, being additionally required as a solvent[3,4]. Thus, the purification of acetic acid is of special interest in the chemical industry.

Acetic acid is a colorless substance having an irritating smell with a boiling point and density of 117.3 °C and 1.0491 g/cm^3, respectively. The production of acetic acid itself yields water as a by-product in several production processes, and thus, water must be removed before it can be used. Although at atmospheric pressure the binary mixture of water and acetic acid does not form azeotrope, the relative volatility of acetic acid to water is very close to unity. Separation through distillation is rather difficult due to tangent pinch at both ends of the vapor liquid equilibrium (VLE) (Figure 1). It is an energy-intensive process from both CAPEX and OPEX viewpoints[5], and it is impractical in some cases due to the requirements of the number of stages and high reflux ratios[6].

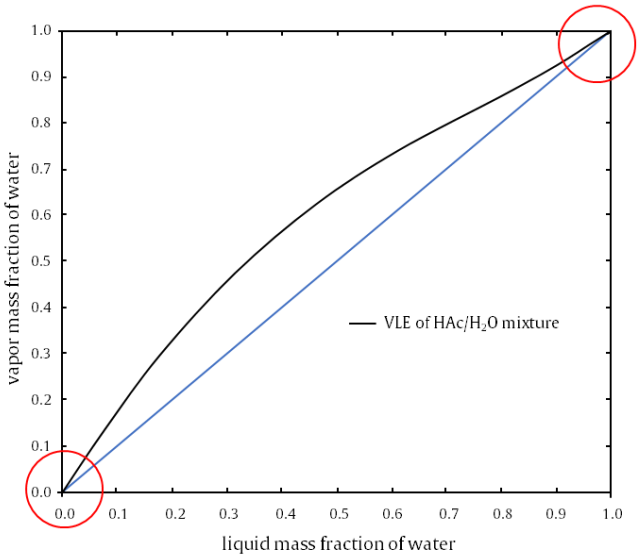

Figure 1. Vapor/liquid equilibrium for acetic acid-water binary mixture (generated from VLE-Calc.com).

Several studies have been reported on HAc/water mixture separation by using advanced processes such as pressure swing distillation, azeotropic distillation, and extractive distillation. Although these processes are applied in the industry, they present some disadvantages. First,

the pressure swing distillation is overlooked since the VLE of HAc/water is not sensitive enough to the pressure[7]. Second, azeotropic distillation involves the addition of a third component to the distillation column to improve the relative volatility and to reduce the separation requirements. This option, among others, provides reduction in the operating costs, but it generates additional steps during the separation and environmental problems due to the presence of a third component[5]. Third, extractive distillation, as an alternative process, usually requires a relative low energy consumption because of low reflux ratio and provides simplification in design and control. However, the binary VLE between the HAc and the different entrainers investigated (e.g., N-methyl acetamide (NMA), N-methyl-2-pyrrolidone (NMP), etc.) also exhibit a tangential pinch as HAc/water mixture, and thus, the energy and capital cost savings compared to conventional distillation process are not attractive[7]. Considering the high energy requirement and/or process complexity of the conventional separation technologies, long time ago, pervaporation has been investigated as a promising technology to separate the HAc/water mixture[3,5,8].

Pervaporation (PV) is a membrane separation technique where one component of a liquid mixture (feed) selectively permeates through a dense membrane. The driving force in pervaporation is the difference in chemical potential across the membrane and it is well represented by the gradient in partial vapor pressure. The permeating component that leaves at the other side of membrane (permeate) is in its vapor state, which is recovered in a condensed form as a liquid[9]. Not only mass transport is involved in PV, but also heat transfer. The heat needed to evaporate the permeate must be transported through the membrane, and this transport of energy is coupled to the transport of matter. The enthalpy of vaporization is taken from the sensible heat of the liquid feed mixture which in turn, reduces the feed-side temperature. The significant advantage of PV is that the process of separation is independent of the VLE. This separation technology is beneficial, where the distillation efficiency mostly lacks, and has excellent potential to be coupled with conventional separation techniques including distillation[8].

As in all membrane processes, the membrane is considered the “heart” of the PV process and it is fundamental for the success of the separation process itself. In developing PV membranes, three critical issues must be addressed and considered: selectivity, productivity, and stability. The chemical and physical properties of the membrane and the interactions of the permeating species with the membrane are crucial for the realization of the separation process. The productivity of the process in terms of flux is influenced by the thickness of the membrane and it is a key factor for the economic viability of the process. The long-term stability of the

membrane is ensured by the chemical and physical properties of the material[10]. Acetic acid, however, is corrosive, and the higher the concentration of HAc in the mixture, the higher is the corrosivity. Thus, it is important to develop a membrane that is acid resistant. In addition, the setup (PV unit) must be appropriate, i.e., both acid and corrosion resistant at the membrane's operating temperature. In a review published by Raza et al.[11], they focused on describing progress in membrane materials (from 2000 to 2020) for the acid-resistant membranes to dehydrate acetic acid/water mixture (polymeric, inorganic, ceramic, and composite membranes). The most critical parameters that control the respective separation by membranes are the membrane material properties, the molecular size of the components and their associated physicochemical properties. Table 1 presents the kinetic diameter, solubility parameters, and polarity for water and HAc.

Table 1. Some properties of acetic acid and water.

Physicochemical property	**HAc**	**H_2O**
Kinetic diameter [nm]	0.43	0.26
Solubility parameter	21.36	47.83
Polarity	6.4	10.2

Several membranes were reported for acetic acid dehydration including both polymeric and inorganic materials, such as polyvinyl alcohol (PVA)[3,12,13], sodium alginate (SA)[14,15], polyphenylsulfone (PPSU)[4], ZSM-5 zeolite[16], MOR zeolite[17], and graphene oxide (GO)[18]. The problem with most of these membranes (like in all membrane applications) is the trade-off between permeance and selectivity. More specifically, for PV membranes, several phenomena may take place during operation which should also be considered during the membrane development. These phenomena are as follows:

1. Swelling of membrane: swelling is an increase in volume of a solid material due to the absorption of liquids or vapors, and degree of swelling is therefore the measure of the dissolution of components in the membrane structure. It is important because in PV, the separation is based on solution-diffusion mechanism. Thus, solubility parameter of the feed components and the polymers are of great importance[19].

   When the concentration of the preferentially permeating component in the feed increases, more of that component will sorb into the membrane, thereby causing increasing swelling. The swelling makes the membrane structure more open, facilitating the permeation of all feed components, and thus, resulting in a higher concentration of non-preferentially permeating components in the permeate, and a decrease separation factor[20].

2. Plasticization: it refers to a change of thermal and mechanical property of a polymeric material. In the case of a membrane, it is caused by an excessive membrane swelling, i.e., the polymer chain spacing (free volume) increases, which results in a severe reduction of selectivity[21]. The plasticization and the coupling effect are correlated when one component is entrained by the diffusion or the sorption of another one. This phenomenon is common in PV, especially for polymeric membranes[22].
3. Coupling effect: in general, coupling is when two objects or molecules interact with each other. A pure component rejected by a membrane can be present in the permeate when it is in a mixture that, in the presence of other component, changes its solubility and diffusivity property (due to coupling effects)[21].
4. Drag effect: Interaction of feed components that leads to an increase in the permeation of the less preferentially permeating component, e.g., dimethyl carbonate (DMC) (C=O) and MeOH (−OH), where MeOH molecules surround DMC and drags through the membrane; it becomes stronger at higher MeOH concentration[21].

Polymeric membranes, aside from the inherent membrane drawback of selectivity and permeability trade-off, commonly suffer in applications with higher temperatures and high acid concentrations. The use of inorganic membranes, on the other hand, shows rather good separation performance (some having surpassed the upper bound trade-off curve between permeability and selectivity for many gas and liquid pairs[23]), but faces the challenge of controlling the pore size of the final separation layer to provide better separation performance and higher acid stability[8]. Moreover, the large-scale application of using inorganic membranes is still limited due to complex fabrication, poor processability, and high capital cost, as compared with polymeric membranes. Hence, membrane development is leaning towards incorporation of stable materials such as inorganic nanofillers into the polymeric membrane to make mixed matrix membranes (MMMs). These membranes usually have better hydrothermal, chemical, and mechanical stability than the pure polymeric or inorganic membranes alone. The challenge, however, in preparation of mixed matrix membranes is to find a suitable pairing of nanofillers and polymer matrix that will improve the separation performance (both permeability and selectivity). To make a good MMM, several criteria are given below for the selection of fillers to be embedded in the polymer matrix.

First criterion is *dispersibility*. The dispersion of the filler into the polymer involves the creation of non-selective interfacial defects, and thus, affects the MMM performance[24]. The nanofillers have high surface energy and tends to agglomerate. Adding them in wet state lessens

agglomeration tendency[25,26]. Most filler particles tend to agglomerate when subjected to common drying methods because of the strong capillary forces between porous particles and their high surface energy, particularly when handled as nanoparticles[24]. A drying-free method was developed by Deng et al. for preparing MMM using ZIF-8 as nanofiller and PVA as polymer matrix for ethanol dehydration[25].

The second criterion is *stability*. The choices for nanofillers are huge and each one of them have different stabilities. For instance, metal organic frameworks (MOFs) have low hydrothermal stability, whereas porous silicates and zeolites, although less compatible with polymers, have better stability in terms of hydrolysis and pH. Due to their stability, only a few MOFs can be used in the preparation of membranes, such as ZIFs, MIL, UiO, and HKUST-1; and among them, Zr-based MOFs are considered to be one of the most chemically stable[27]. Regardless of their Si/Al ratios, zeolites tend to be stable under hydrothermal conditions up to 200 °C, which can be important for stable PV operation at higher temperatures[24]. However, the acid stability of zeolite membranes is enhanced with increasing Si/Al ratio in the framework. Therefore, zeolite membranes with medium Si/Al ratio are preferred for the dehydration of carboxylic acidic mixtures (Figure 2), such as acetic acid/water[28,29].

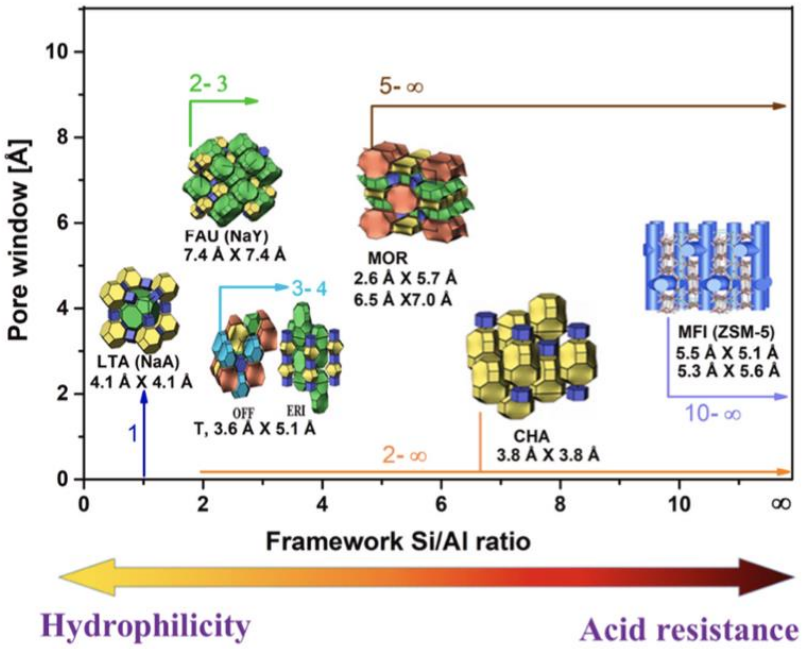

Figure 2. Attributes of various zeolite frameworks with pore size, hydrophilicity, and acid stability trend[8].

The third criterion is the *hydrophilicity/hydrophobicity*. In MOFs, the hydrophobic or hydrophilic nature is mainly defined by the ligands and by the presence of open metal sites. Some examples of hydrophobic MOFs are ZIF-8 and ZIF-71. By contrast, UiO-66, MIL-101(Cr), and HKUST-1 are highly hydrophilic. In addition, some other inorganic materials,

such as zeolites (KA, NaA, CaA, NaX, NaY, silicate-1, and H-ZSM-5), graphene, porous silicas, and TiO_2 tend to be hydrophilic as well[24]. The nanofillers can also be functionalized with hydrophilic or hydrophobic groups to increase their affinity with the polymeric matrix[30]. The addition of nanofiller can modify the intrinsic hydrophilicity/hydrophobicity of the polymer matrix depending on the type of material[31].

Fourth criterion is the *size* of the filler, which needs to be considered because it dictates the surface properties of the nanofillers. Structural defects of the membrane can be due to the filler size which affects the dispersion. Incorporation of nano-sized fillers as adsorbent in dense membrane improved the performance (flux and selectivity) in both gas separation and pervaporation for several types of feed mixtures[32-33]. In general, the smaller the size of the filler, the thinner is the filled membrane. Fillers with micron size will inherently give thicker filled membranes than that of unfilled membranes. MMMs made by incorporating hydrophilic fillers of micron sizes show low water selectivity at higher filler loading because of defects in the polymer–filler interface due to poor polymer–filler compatibility. In contrast, nanosized filler may contribute to improve the flux and selectivity of a MMM, even at a much lower concentration than fillers of micron size[34]. However, nanosized filler, as mentioned above, is very difficult to mix with a polymer because of its agglomeration tendency.

Lastly, the *particle morphology and pore size* also determine MMM feature[24]. For example, if the pore size lies between the molecular kinetic diameters of the target components in the mixture to be separated, the smaller molecule can diffuse into the pores, while the larger molecule is retained, causing a molecular sieving effect. However, if the pore size is slightly larger than the diameter of the larger molecule, the separation is based on the difference in diffusion rates. Moreover, if the pore size is vastly larger than both molecules, they can be separated principally by the difference in their adsorption properties[35]. Kulkarni et al. reported the increase of both permeability and selectivity as the zeolite content increases. Those results were explained by the enhancement of hydrophilicity, selective adsorption, and the establishment of molecular sieving action in the dehydration of acetic acid using pervaporation[23].

Studies using mixed matrix membranes for dehydration of acetic acid by pervaporation have been published using different polymers and nanofillers (Table 2). These studies reported that MMMs resulted in improvement of flux and selectivity as compared to the neat polymers.

Table 2. Mixed-matrix membranes reported for dehydration of acetic acid by pervaporation.

Polymer	Nanofiller	Nanofiller loading (%)	Permeate pressure (mbar)	Membrane thickness (μm)	Temperature (°C)	HAc in feed (wt %)	Permeate flux (kg/m^{2}h)	Separation factor (-)	Reference
PEI	NH_2-UiO-66	20	1	< 10	60	95	0.212	356	[36]
PVA	Fullerenol	5	1	1.5	40	90	0.087	216	[3]
PPSU	Silica	0.5	< 2.5	< 2	70	70	2.34	3.3	[37]
All silica zeolite	Silica	100	2	3	75	90 50	0.23 0.56	1700 >10 000	[38]
PVA + CMC + MA	Bentonite	2	-	60	35	97	0.05	366	[12]
PANBA	Na-MMT	0.5	-	50	30	99.5 71.7	0.052 0.173	1473 102	[34]
PVA/PAA	AgNP	2.25	< 10	50	40	20	0.23	22	[13]
PVA	NaY zeolite	15	13.3	40	30	50 90	0.15 0.08	99 2423	[23]

*Acronyms: PEI (polyether imide), CMC (carboxymethyl cellulose), MA (maleic acid), PANBA (poly(acrylonitrile-co-butylacrylate)), Na-MMT (sodium montmorillonite), PAA (polyacrylic acid), AgNP (silver nanoparticle)

Table 3. MMMs based on poly(ether ketone), poly(ether ketone), and their derivatives.

Polymer	Nanofiller	Application	Mixture System	Reference	Relevant Findings/Remarks
PEEK-WC	CuNi-MOF	GS	CO_2/N_2 CO_2/CH_4 O_2/N_2 H_2/N_2	[26]	• E_{mod} and break strength ↑ as MOF ↑ (for PEEK-WC); thermal properties are not affected with changing MOF concentration • CuNi-MOF has good adhesion with PEEK-WC • ↑ MOF, ↑ Permeability of gases (mainly due to ↑ D as S is almost constant)
PEEK-WC	Modified NaA zeolite (SAR =1)	GS	O_2/N_2 CO_2/N_2	[31]	• NaA-DEA increases hydrophilicity, whereas NaA-APDEMS decreases it (presence of terpene resin promotes hydrophobicity) • NaA-DEA has better affinity with the polymer • All MMMs show lower permselectivity values with respect to the pure polymer.
PEK-C	ZIF-8	PV	H_2O/MeOH/MTBE	[39]	• Hydrophilicity increased; mechanical properties decreased slightly with increase in ZIF-8 loading • The MMMs show good structural integrity after pervaporation experiments. • MMM with 4 wt% ZIF-8 loading has max. values of PSI and selectivity of 2.92×10^4 and 1.4×10^5
SPEK-C	STA/PVA/GA**	PV	HAc/H_2O	[40]	• The composite membrane has a flux of 0.592 kg/m^2 h and a separation factor of 91.2 at a feed water content of 10 wt%.

*Acronyms: GS (gas separation), SAR (Si/Al ratio), STA (silicotungstic acid), GA (glutaraldehyde), MTBE (methyl tert-butyl ether)

***not a nanofiller but used as a modifier to make a composite membrane.*

This paper focuses on PEEK-WC (poly(oxa-p-phenylene-3,3-phthalido-p-phenylene-oxa-p-phenyleneoxy-phenylene) as polymer matrix. It is a modified poly(ether ketone) with a cardo (lactone) group attached to the backbone (Figure 3). It is an amorphous polymer with the same good thermal and mechanical properties and chemical resistance of PEEK and PEK (polyether ketone) and its advantage is the higher solubility in organic solvents. The presence of the cardo group reduces the degree of crystallinity, thus making PEEK-WC more soluble in some chlorohydrocarbon solvents such as chloroform and in polar organic solvents such as dimethyl formamide (DMF), *N*-methyl pyrrolidone (NMP) and tetrahydrofuran (THF), and in non-polar dichloromethane (DCM). This amorphous glassy polymer has a glass transition temperature of 225 °C making it an interesting candidate for preparing membranes that can resist high temperatures. PEEK-WC could be produced by condensation reaction between phenolphthalein and bis(4-nitrophenyl) ketone (DNBP)[19].

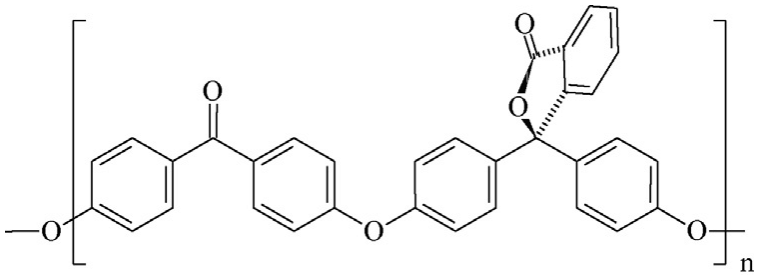

Figure 3. Structural formula of PEEK-WC.

PEEK-WC presents high selectivity values (e.g., mixtures of EtOH/cyclohexane[19], MeOH/MTBE[41]) but low permeability to be interesting as a membrane material for industrial applications. For this reason, different researchers have tried to improve the permeability without affecting the selectivity by means of nanoparticle addition[26]. For gas separation applications, studies involving mixed matrix membranes based on PEEK-WC are already present. Clarizia et al. reported the embedding of NaA (LTA) zeolite into the PEEK-WC membrane matrix. They modified the zeolite surface with different coupling agents, such as γ-aminopropyl-diethoxymethyl silane (APDEMS) and diethanolamine (DEA), to improve the filler-polymer affinity. However, at high zeolite concentration, the gas separation performance of the MMM was lower than that of the neat polymer[31]. Some methods have been developed to further improve the adhesion of PEEK-WC for 3D-mesoporous nanoparticles. For example, the MIL-101 was functionalized with a sulfonic acid group to increase the affinity with the polymer matrix[42]. The resulting membranes have shown an improved CO_2 permeability and CO_2/gas selectivity. The increased selectivity was mainly attributed to the increased polar interaction between CO_2 and sulfonic acid groups, as well as the good filler–polymer interface

compatibility. In a recent paper, Esposito et al.[26] studied the impact of the polymer matrix on the effectiveness of same MOF when it is embedded in a glassy (PEEK-WC) or a rubbery (PEBAX® 1657) polymer. The addition of CuNi-MOF increased the mechanical strength (Young's modulus and break strength) with MOF content, but thermal properties were not affected. The permeability of gases also increased by increasing MOF content, the results were attributed to the increased gas diffusivity, while sorption coefficient remains almost constant. The enhanced diffusion clearly indicates transport within the pore structure of CuNi-MOFs, which increases the total free volume of MMMs, promoting the gas diffusion for all gases.

Mixed matrix membranes based on PEEK-WC for HAc/water separation by pervaporation have not yet been reported up to date, but there are studies done on PEK and SPEK (sulfonated polyether ketone) derivatives, particularly with the presence of a cardo group[39,40] on gas separation and pervaporation of other solvent mixtures (Table 3).

2. Objectives

The main objective of the work is the development of new polymeric membranes, loaded with nanomaterials, with good chemical resistance against organic acids, in particular, acetic acid. Specifically, polyether ether ketone modified with a cardo group (PEEK-WC), will be employed for the production of dense membranes. The incorporation of specific nanomaterials, such as MOFs, within the membrane matrix will be investigated. Several nanofillers will be incorporated in the PEEK-WC membrane to identify the most suitable one that will improve the permeance without compromising the selectivity. The prepared membranes will be characterized from a physicochemical point of view and investigated for the dehydration of acetic acid by pervaporation.

The specific objectives of this work are as follows:

1. Prepare and characterize PEEK-WC films with thicknesses less than 10 μm;
2. Synthesize and characterize different nanofillers, particularly, metal-organic frameworks (MOFs), such as ZIF-8, HKUST-1, and MIL-101(Cr);
3. Incorporate the different nanofillers (2.5 and 5.0 wt%) into the PEEK-WC polymer to prepare MMM films with thicknesses less than 10 μm;
4. Characterize the MMMs in terms of morphology, mechanical and thermal properties, wettability (contact angle) and solvent resistance (swelling); and
5. Perform pervaporation tests with the MMMs to investigate the separation performance (permeance and selectivity) of membranes for the dehydration of acetic acid.

Characterization of the nanofillers will include XRD (X-ray diffraction), TGA (Thermogravimetric analysis), SEM (Scanning electron microscopy), and microporosity analysis. The addition of different MOF nanofillers within the membranes will be evaluated with the aim of producing MMMs able to combine the benefits from both the polymer and the inorganic materials, like: (i) improving the mechanical resistance of the membranes; (ii) increasing the selectivity of the membrane towards target species; and (iii) enhancing membrane permeability.

3. Experimental

3.1. Materials

The polymer PEEK-WC (M_w = 224,000) was supplied by Chanchung Institute of Applied Chemistry (Academia Sinica, China). The reagents $Zn(NO_3)_2{\cdot}6H_2O$ (98%), $Cu(NO_3)_2{\cdot}2.5H_2O$ (98%), $Cu(NO_3)_2{\cdot}3H_2O$ (99%), $CrCl_3{\cdot}6H_2O$ (96%), terephthalic acid (96%), and trimesic acid (95%) were all purchased from Sigma-Aldrich and were used as obtained. Acetic acid (99.8%) and chloroform (99%) were purchased from Acros Organics.

3.2. Methodology

3.2.1. Membrane preparation

PEEK-WC was dissolved in chloroform to obtain 10 wt% of polymer. Once solubilized, the polymer solution was left to degas overnight. The solution was casted on a glass plate using Elcometer 4340 Automatic Film Applicator with varying casting thickness (100 – 250 μm) to make membranes with different thickness. The solvent was left to evaporate completely for at least 5 h. Then, the glass plate was soaked in water bath overnight to allow the membrane to detach from the glass plate. The membrane was then dried in the oven at 50 °C for 4 h. After drying, the thickness was measured using a Baxlo 4000/Film thickness gauge micrometer ($\pm$0.001 mm).

3.2.2. MOF nanofillers synthesis

For the synthesis of the metal-organic framework nanofillers, several methods from literature have been tried to check which one will give small (< 200 nm) and monodisperse nanoparticles with an appreciable yield. These methods were also chosen based on whether they used solvent- or aqueous-based synthesis, and their non-complexity.

3.2.2.1. ZIF-8

In a typical ZIF-8 synthesis, a solution of $Zn(NO_3)_2{\cdot}6H_2O$ (98%, Sigma-Aldrich) in distilled water is rapidly added to a solution of 2-methylimidazole (Hmim) in distilled water (the molar ratios of the reactants are listed in Table 4). The mixture turns from colorless to milky white and the rate of color change depends on the molar ratio of the metal and the ligand. The mixture is stirred for a certain period at room temperature. The solid is separated by centrifugation (10 000 rpm, 10 min) and washed with solvent, and once with chloroform for the final wash. Then, the product, a white powder, is dried overnight at 60 °C.

Table 4. Synthesis conditions for ZIF-8.

Sample ID	Zn^{2+}:Hmim:H_2O	Solvent for		Synthesis time	Yield (%)	References
		reaction	washing (3X)			
Z1	1:60:2228	water	methanol	4 h + 16 h**	>98	[43]
Z2	1:150:2228	water	methanol	2 h + 16 h**	>98	modified Z1
Z3	1:150:2228	water	methanol	2 h	95	modified Z2
Z4	1:8:500	water	water (2X), ethanol (1X)	30 min	96	[44]
Z5	1:70:1238	water	water	5 min	20	[45]

*all washing was done 3X (for Z4, twice with water and once with ethanol).
**with 16h incubation in oven at 95 °C after mixing, and before centrifugation and washing.

3.2.2.2. HKUST-1

For the synthesis of this MOF, $Cu(NO_3)_2 \cdot 2.5H_2O$ and benzene-1,3,5-tricarboxylic acid (BTC) were dissolved in a known amount of solvent (Table ***5***). The solution was stirred for 24 h (or 1 h) at room temperature and the final product, a blue powder, was collected by centrifugation (10000 rpm, 10 min) and washing with solvent (or a mixture of solvent), and a final wash with chloroform. Then, the product was dried at 100 °C overnight.

Table 5. Synthesis conditions for HKUST-1.

Sample ID	Cu^{2+}:BTC:EtOH	Solvent for		Synthesis time	Yield (%)	References
		reaction	washing (3X)			
H1	1.7:1:120	ethanol	water (2X), ethanol (1X)	24 h	33	[46]
H2*	1.8:1:120	ethanol	water (2X), ethanol (1X)	24 h	33	[47]
H3	1:2:2222	water	water:ethanol (1:1 v/v)	1 h	25	[48]
H4	1.7:1:120	ethanol	water (2X), ethanol (1X)	1 h	31	modified H1

*Precursor used is $Cu(NO_3)_2 \cdot 3H_2O$; for all the other methods, $Cu(NO_3)_2 \cdot 2.5H_2O$ was used as precursor.

3.2.2.3. MIL-101(Cr)

MIL-101(Cr) was synthesized at 200 °C for 15 min under microwave irradiation. The molar compositions of the reactant mixture consisting of $CrCl_3 \cdot 6H_2O$, terephthalic acid (TPA), and water are shown in Table 6. The reactant mixture was loaded into a Teflon autoclave, sealed, and placed in a microwave oven (Ethos PLUS High-Performance Microwave Labstation). The autoclave was heated at 200 °C in 5 min and kept at this temperature for another 15 min. After, the autoclave was cooled down to room temperature, and the solids were collected by centrifugation, washing, and drying. The final product, a green powder, was obtained after purifying the solids to remove free acid by DMF treatment for 1 h at 70 °C.

Table 6. Synthesis conditions for MIL-101(Cr).

Sample ID	Cr^{3+}:TPA:H_2O	$pH_{initial}$	Solvent for		Synthesis time	Yield (%)	References
			reaction	washing (3X)			
M1*	1:1:250	5-6	water	water	15 min	46	[49]
M2	1:1:250	2-3	water	water	15 min	<2	[49]

*NaOH (10 N) solution was added to obtain initial pH.

3.2.3. Mixed-matrix membranes (MMMs) preparation

Two nanofiller concentrations were used: 2.5 and 5.0 wt% by polymer. The MMMs were prepared as follows. Firstly, PEEK-WC polymer was dissolved in chloroform with the amounts listed in Table 7. Then, the nanofiller was dispersed in chloroform by sonication for 2 h before mixing it with the PEEK-WC solution. The amount of filler and polymer was kept constant at 1 g, and the weight proportion of solvent: (filler + polymer) mixture was maintained constant at 90:10. The mixture was stirred for 24 h to ensure homogeneous nanofiller dispersion and obtain the MMM solution. After stirring, the MMMs were prepared in the same way as the bare PEEK-WC membrane described in section *3.2.1*. The MMMs are labeled as M*X*-*Y*, where *X* is the MOF (Z: ZIF-8, H: HKUST-1, and M: MIL-101), and *Y* is the nanofiller content.

Table 7. Preparation of MMMs.

Filler content (%)	PEEK-WC solution	Nanofiller solution
2.5	0.975 g in 6.5 g $CHCl_3$	25 mg in 2.5 g $CHCl_3$
5.0	0.950 g in 6.0 g $CHCl_3$	50 mg in 3.0 g $CHCl_3$

3.2.4. Characterization

The nanofillers were analyzed by X-ray diffraction (XRD) to confirm their crystallinity and structure. The analyses were carried out at ambient temperature using Malvern Panalytical Empyrean. Simulated PXRD pattern were calculated from single crystal data with the MERCURY 3.0.1 software suite from CCDC.

Nitrogen physisorption isotherms of the nanofillers were measured at 77 K using a Micromeritics ASAP™ 2020 System. Prior to the analysis, samples were outgassed with a heating rate of 10 °C/min until 110 °C and a hold at that temperature for 12 h. The BET (Brunauer−Emmett−Teller) specific surface area was determined from the nitrogen adsorption isotherms.

The nanofillers and the MMMs were characterized by scanning electron microscopy (SEM) using SEM-FEG Inspect F50. For sample preparation, the membranes were immersed in liquid nitrogen and then fractured. The powder samples were mounted on carbon tape and coated with Pd using a Leica sputter coater. Energy Dispersive X-ray (EDX) mapping was also done to the membrane samples to check the nanofiller distribution across the polymeric matrix. For this purpose, the membrane samples were coated with carbon.

Thermogravimetric analyses (TGA) were conducted using a Mettler Toledo TGA/SDTA 851e system to check the thermal stability of the nanofillers and the nanofiller content in the

mixed matrix membranes. Samples of about 5–10 mg were placed in an alumina crucible and then heated from 35–800 °C at a heating rate of 10 °C/min under nitrogen flow.

3.2.4.1. Contact angle measurements*

The wettability of the PEEK-WC based membranes was measured by the water contact angle method using a CAM 200 KSV (Finland) instrument. Five measurements were carried out on both sides (top and bottom) of each membrane and the average and standard deviation were calculated.

3.2.4.2. Mechanical tests*

The mechanical properties of the membranes were measured using a Zwick/Roell Z 2.5 test unit at ambient temperature (25° C). Each membrane sample (1×5 cm) was stretched unidirectionally at a constant speed of 5 mm/min. For each membrane at least five sample were analyzed, and the average and standard deviation were calculated.

3.2.4.3. Degree of Swelling (DS)

The solvent/water mixture uptake of the membranes was investigated in acetic acid solutions at different concentrations. Strips of membrane (3×2 cm) were cut and weighed, w_D. Then, the membrane strips were soaked in the solutions (0, 20, 40, 60, and 80 wt% HAc) at 50 °C for 3 days to reach the membranes swelling equilibrium. Then, the membrane strips were taken out, wiping the surface quickly with tissue paper, and immediately weighed again, w_W. A digital microbalance ($\pm$0.001 mg) was used to weigh the samples. Based on the weight of the absorbed solvent, the degree of swelling, DS, was calculated for each solution as follows:

$$DS\ (\%) = \frac{w_W - w_D}{w_D} \times 100$$

3.2.5. Pervaporation Experiments

The pervaporation tests were performed with two initial HAc/water solutions (85/15 and 95/5 %w/w) in the laboratories of DeltaMem AG. The effective membrane area in each cell is 38 cm^2. The mixture was filled into a feed tank and recirculated by a pump with a feed flow parallel to the membrane surface. The feed goes to the membrane cells, and then, the product from the cells is returned to the feed tank as retentate. A heating system maintains constant the feed/retentate temperature at 70 °C. In the permeate side, a vacuum of 10 mbar was maintained by a vacuum pump. Permeate samples were collected in a cold trap with dry ice and ethanol mixture. For each measurement point, the amount of permeate, time, as well as the feed/retentate samples were collected.

**Characterization was done by CNR-ITM.*

4. Results and Discussion

4.1. MOF Synthesis and Characterization

ZIF-8

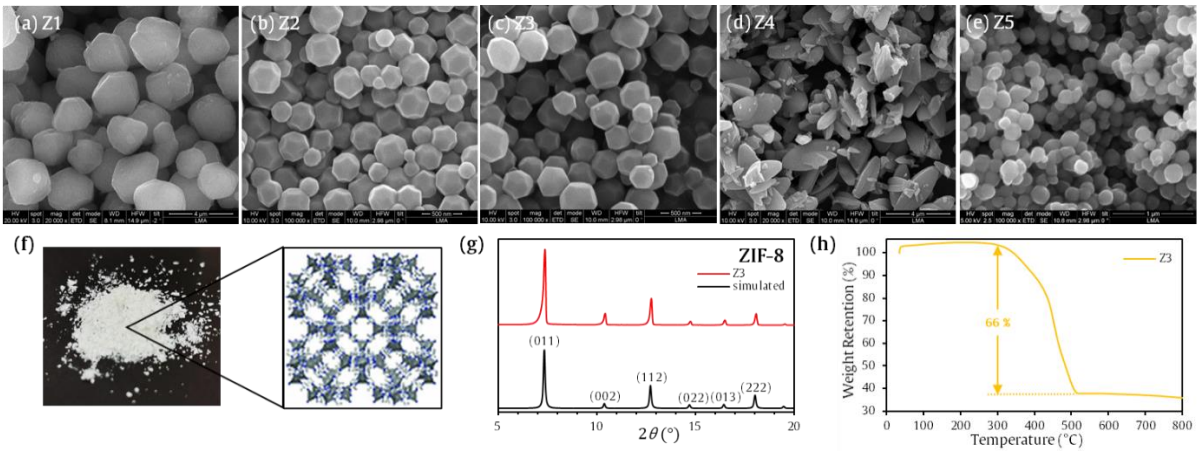

Figure 4. (a-e) SEM images of ZIF-8 samples, (f) as-synthesized ZIF-8 image with structure, (g) PXRD pattern of the as-synthesized Z3 sample and simulated ZIF-8; and (h) TGA plot of Z3.

For the synthesis of ZIF-8, several methods available in literature has been used and/or modified. Firstly, both Z1 and Z2 give a yield of >98% (Table 4). The particle size of Z1 is about 2.5±0.5 μm (Figure 4) which is too big to be used as a filler for a 10-μm membrane. Thus, the Zn/Hmim ratio was increased from 1:60 for Z1 to 1:150 for Z2 which, in turn, gave particles with size of 300±100 nm. The method for Z2 synthesis includes 16 h of oven incubation at 95 °C, whereas this step was removed for Z3. The yield for Z3 is 95% and its particle size is 315±150 nm. Methods involving short synthesis times have been used as well. *Karimi et al.* used Zn/Hmim ratio of 1:8 with a synthesis time of 30 min (Z4). Although this method gives a yield of 96%, the product did not have the sodalite (SOD) topology (Figure 4).

In ZIF-8 synthesis, the reaction stoichiometry between the zinc precursors and 2-methylimidazole (Zn/Hmim) should be 1:2. However, *Cravillon et al*. found that the addition of excess 2-methylimidazole was necessary in the aqueous solution because the deprotonation processes of 2-methylimidazole are difficult because of its high pK_a value in the aqueous solution as compared to when organic solvents are used[50]. Finally, Z5 was synthesized using the method by Pan *et al.*[45] with a synthesis time of 5 min. The particle size is 150±70 nm, which is a good size for a nanofiller for a 10-μm membrane. However, its yield is very low.

For the synthesis of MMM, Z3 was used as nanofiller because of the size of nanoparticle and yield. The PXRD pattern of Z3 agrees with the simulated ZIF-8 pattern (Figure 4), showing all the characteristics peaks indicating that the obtain product is a pure crystal. The TGA analysis (Figure 4) reveals structural stability of Z3 up to 300 °C with a weight loss of about 66%.

HKUST-1

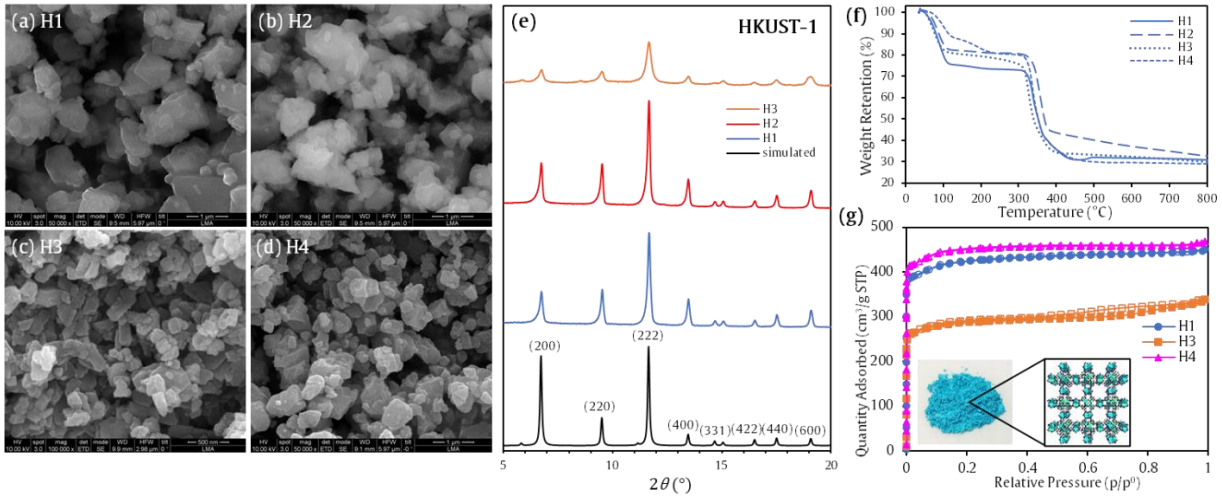

Figure 5. (a-d) SEM images, (e) PXRD patterns, (f) TGA plots, and (g) N_2 sorption isotherms of HKUST-1 samples.

The synthesis methods for nanosized HKUST-1 gave a yield of less than 40% (Table 5). Unlike ZIF-8, the morphologies of the synthesized HKUST-1 nanoparticles (Figure 5) are not homogeneous in size (~74–900 nm), and they are irregular (they do not have the octahedron-shaped morphology of micro-sized HKUST-1). For HKUST-1, an accurate control of crystallite dimensions is problematic due to: i) fast crystallization kinetics and ii) constant nucleation[51]. This was also observed by Wee *et al.*[47] from which the method was adapted for H1 and H2 synthesis. Smaller particle sizes are seen for H3 because of shorter synthesis time, although the reaction mixture's molar ratio is different. For the synthesis of H4, the reaction mixture of H1 was used, but the synthesis time was shortened from 24 h to 1 h. This gave particles of smaller sizes (~40–270 nm) as well (Figure 5). For all synthesis conditions, it can be noticed that smaller particles are growing on the surface of bigger particles as a consequence of constant nucleation.

Despite the irregularly shaped crystals, H1 and H2 showed good crystallinity as evidenced by their PXRD patterns (Figure 5) agreeing with the simulated one. For H3, however, the PXRD peaks are less intense due to the different Cu:BTC ratio. The stoichiometric ratio for the synthesis of HKUST-1 from a balanced reaction is 3Cu:2BTC. This also explains why the yield for H3 is the lowest.

All HKUST-1 samples show two decomposition regions (Figure 5): the first one corresponds to the evaporation of physically adsorbed solvent (water/EtOH) and the second one, at around 325 °C, corresponds to the decomposition of the HKUST-1 framework. The residual solids are Cu, Cu_2O, and CuO. An additional region is observed for H1 and H4 (more

prominent for H4) around 120 – 220 °C due to release of water that is chemically bonded on copper atoms, and solvent that is physically adsorbed in the internal pores.

All samples reached the adsorption equilibriums in the low-pressure region, and except for H3, they exhibit no hysteresis loops at high-pressure region (Figure 5. (a-d) SEM images, (e) PXRD patterns, (f) TGA plots, and (g) N2 sorption isotherms of HKUST-1 samples.). This is a characteristic of a Type I isotherm indicating microporous structure of the samples (<2 nm). Table 8 shows the surface area and pore volume of the different MOFs synthesized in this work. Except for H3, all values are comparable to those reported in literature. The hysteresis loop, and the low values of surface area and pore volume for H3 might be due to either its low crystallinity and/or presence of impurities occluding the pores such as residual BTC that were not removed during the evacuation stage before the sorption measurements. In contrary, H4 gave the highest values of both surface area and pore volume, which supports the TGA analysis results, where an additional region of weight loss was observed indicating presence of more pores. Thus, H4 was used for the synthesis of the MMM.

Table 8. Textural properties of the different MOF samples*.

Sample ID	S_{BET} (m^2/g)	$S_{Langmuir}$ (m^2/g)	V_P (cm^3/g)	V_m (cm^3/g)
H1	1145 ± 32**	1914 ± 2	0.639	0.597
H3	933 ± 23**	1280 ± 5	0.433	0.401
H4	1458 ± 37**	1996 ± 4	0.683	0.653
M1	2713 ± 17	-	0.977	0.311

*V_p: total pore volume at ~0.99 p/p^0, V_m: micropore volume by t-plot analysis.
**BET constant, C < 0 (See Figure A2 for the BET isotherm linear plots)

MIL-101(Cr)

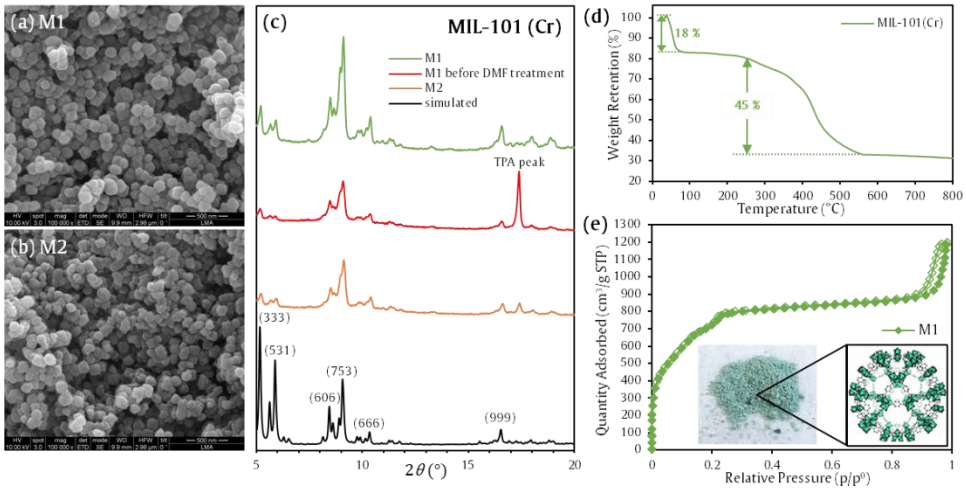

Figure 6. (a-b) SEM images, and (c) PXRD patterns of MIL-101(Cr) samples; and (d) TGA plot, and (e) N_2 sorption isotherm of M1.

The microwave (MW) irradiation method was used for the synthesis of MIL-101(Cr) because it is faster and gives smaller particles. The initial pH of the reaction mixture was varied

because it was reported[52] that increasing the pH promotes the production of chromium trimers (with decreasing monomer), as well as the deprotonation of TPA into benzenedicarboxylate which are both needed for the synthesis of MIL-101 structure.

In Figure 6, the particle sizes of M1 and M2 did not differ much but the yield for M2 is considerably low as there were many free acids in the product. The surface of the particles of M1 are smoother and more defined than that of M2 denoting that the formation of the crystal structure in M1 is better. It is also supported by the PXRD result (Figure 6) where M2 shows less intense peaks as compared to M1. The PXRD pattern of M1 before the DMF post-treatment shows a strong peak at around 17° which corresponds to TPA peak which shows that the post-treatment with DMF is important to obtain a pure product.

The TGA plot of MIL-101(Cr) shows structure stability up to 250 °C (Figure 6). Two weight-loss stages are observed: the first, corresponding to 18%, which is due to loss of guest water molecules; the second (45%) is due to the leaving of OH/F groups[53] and the decomposition of the framework. The residual solid is Cr_2O_3.

The N_2 sorption isotherm (Figure 6) of the as-synthesized MIL-101(Cr) is of type I with secondary uptakes around p/p^0 = 0.1 and p/p^0 = 0.2, indicating presence of two kinds of microporous windows. The existence of hysteresis in the isotherm indicates the presence of mesopores in the sample which corresponds to the larger cages of this framework (Figure A1).

4.2. Membrane Characterization

SEM

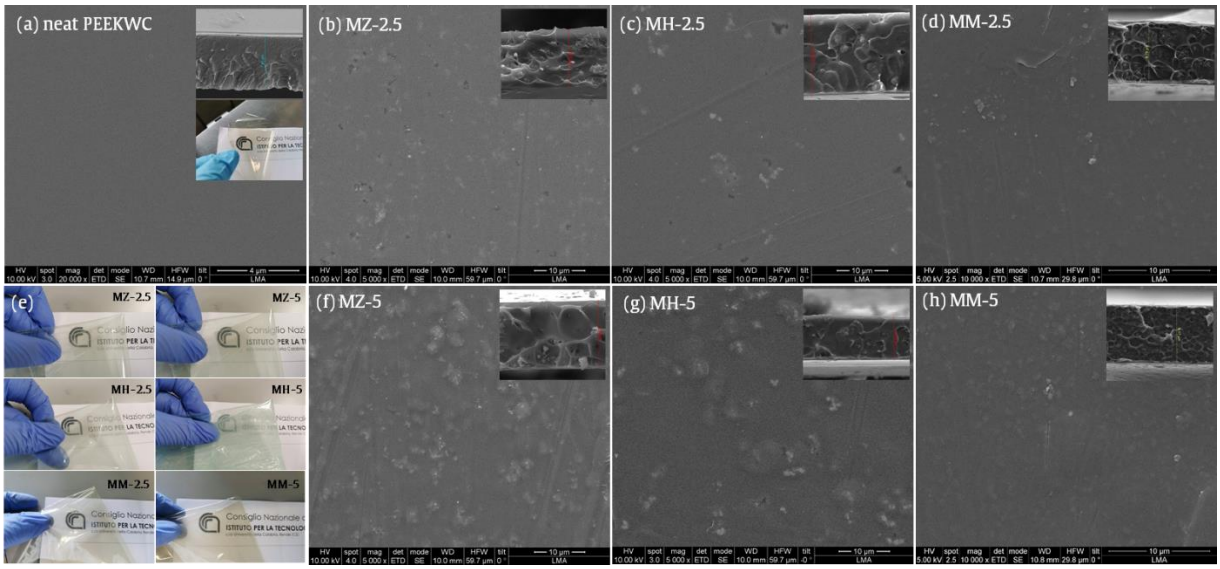

Figure 7. SEM images of (a) PEEK-WC, (b-d) MX-2.5, (e) physical appearance of MMMs, and (f-h) MX-5; membranes' cross-sections are on the insets; for the neat PEEK-WC, its physical appearance is also on the inset.

As the membranes are dense films, there are not much notable features to see in their morphology except when the nanofillers were added (Figure 7). Most of the fillers are embedded across the membrane thickness but some of them can also be seen on the surface (especially at higher nanofiller content, Figure 7). No discontinuities (i.e., pinholes) are seen in the membranes indicating that they are defect-free. The SEM images of the cross-sections confirmed that the membranes are less than 10-μm thick. The EDX mapping of the MMMs show good dispersion of the nanofillers (Figure A3). The films are almost transparent and the opacity of the MMMs slightly increased when the nanofiller content was increased.

TGA

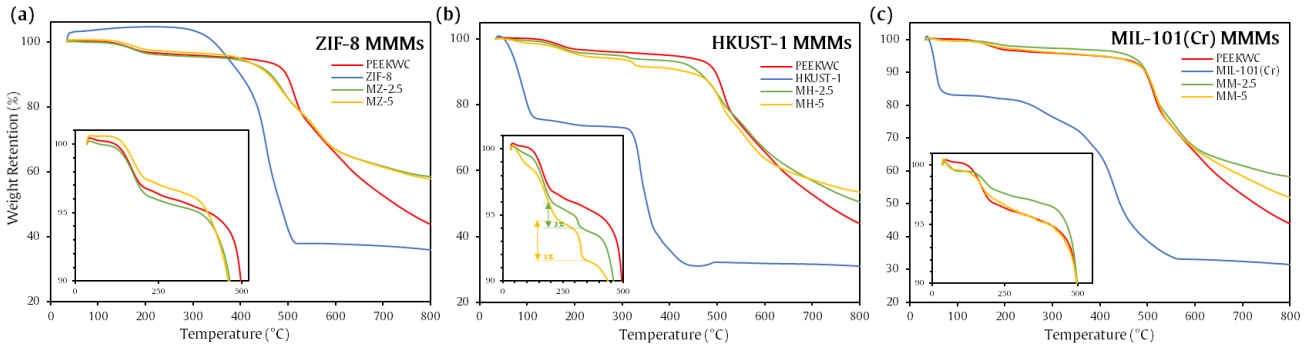

Figure 8. TGA plots of MMMs.

MZ membranes degrade at a lower temperature (375 °C) compared to the neat polymer (500 °C). Similar result is observed for MH membranes (450 °C), whereas for MM membranes, the degradation temperature is the same with the neat polymer. The total weight loss up to 800 °C is less for all MMMs as compared to neat polymer because of the residual oxides from the MOFs. The actual filler content was calculated for MH membranes as shown in Figure 8 because the degradation of HKUST-1 shows a sharp decline in weight loss, thus making distinct the effect of the filler on the TGA plots of the MH membranes. However, it is difficult to do the same estimation for MZ and MM membranes. Nevertheless, all membranes have good thermal stability.

Mechanical properties and contact angle measurements

The addition of nanofillers, in general, improved the stiffness of the PEEK-WC membrane (Figure 9), and decreased its elasticity (Figure 9). This is expected for mixed-matrix membranes because the nanofillers act as reinforcements on the polymer matrix. They provide rigid points which hinder further polymer chain mobility, making it less flexible. However, MM membranes became less stiff as the filler content increased.

The tensile strengths of the MMMs (Figure 9) are all lower than the pure PEEK-WC which may indicate possible incompatibility between the filler and the matrix (at the interface), creating points that accelerate the failure of material. For MZ membranes, the increase in filler content decreased the tensile strength of the MMM. This is explained by the embrittlement of the membranes as shown by the decrease in ductility (Figure 9). The same trend is seen for MM membranes. However, an opposite trend is observed MH membranes, indicating that filler-matrix incompatibility increases with filler content. In terms of mechanical property, it shows an interesting approach to explore other filler types and contents for the optimization of mixed matrix membrane properties.

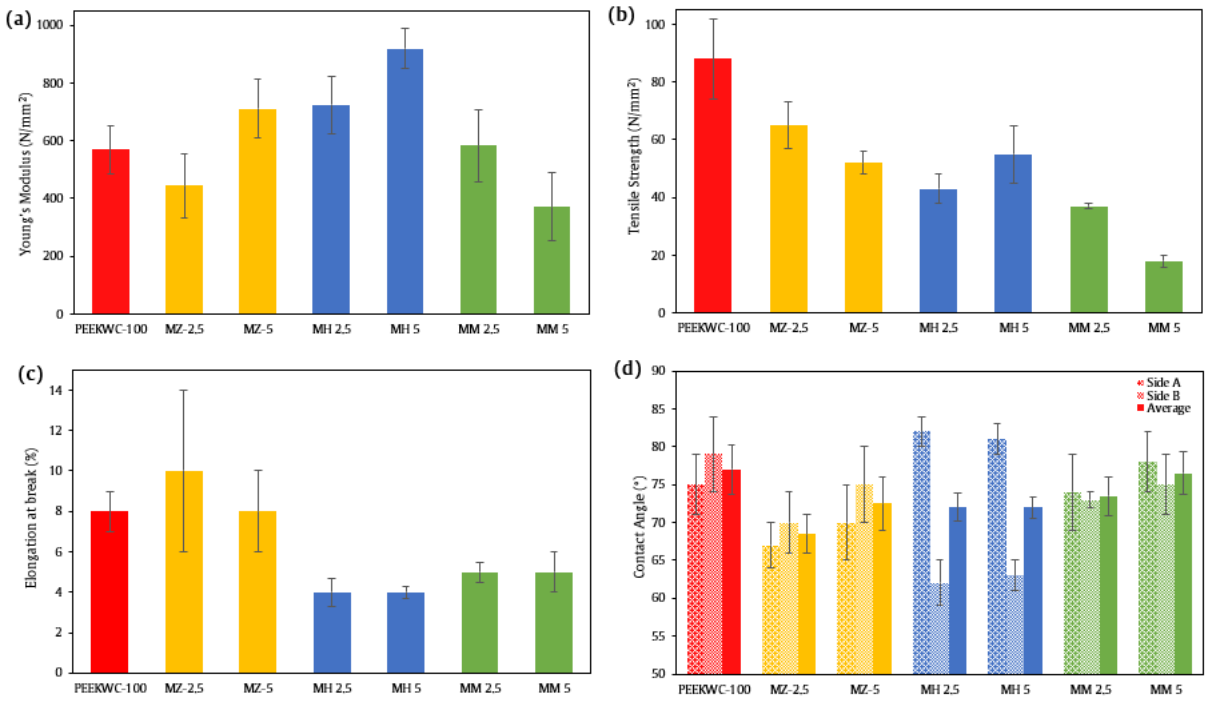

Figure 9. (a-c) Mechanical properties, and (d) water contact angle results (Side B is the substrate-facing side).

All MMMs, as well as the pure PEEK-WC membrane, are slightly hydrophilic (<90°) in nature (Figure 9. (a-c) Mechanical properties, and (d) water contact angle results (Side B is the substrate-facing side).) which means that a polar component can permeate easier through the membrane than a nonpolar component. Because the contact angle depends on chemical nature and roughness of surface, the measurements were carried out in both side of membranes, and thus, for excluding artefacts (like small defects on the surface) and for easy understanding, average values were calculated. In terms of average values, the contact angle decreased (relative to neat PEEK-WC) when the nanofiller content is 2.5 wt%. An increase in nanofiller content to 5 wt% increases the contact angle. Nevertheless, the contact angles for both cases are still lower than that for the neat PEEK-WC.

Based on the results, the addition of hydrophobic nanofiller does not necessarily mean that the membrane becomes more hydrophobic and likewise, the addition of hydrophilic nanofiller makes the membrane more hydrophilic. The water contact angle of a material is driven by not only the chemical make-up of the material, but also by the surface roughness, as described above. The air trapped in the space between the MOF particles is an important contributor to the increased hydrophobicity as the water contact angle of air is considered to be 180°[54]. Thus, the increased surface roughness arising from the individual MOF crystals is the main contributor to the increased contact angle of the MMMs as the filler content is increased. Due to the irregularity in the morphology of HKUST-1 particles, as compared to the other two MOFs, it is possible that there are more particles present on the air-facing side of the MMM film (Side A). This increases the roughness which in turn increases the contact angle of Side A of MH membranes.

Membrane Swelling

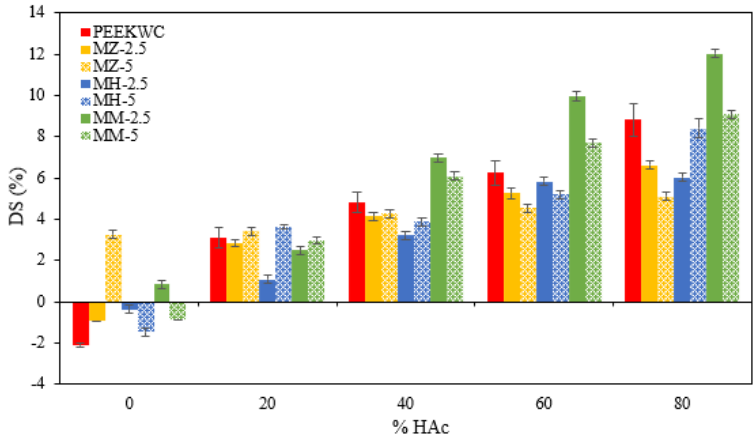

Figure 10. Swelling degree of PEEK-WC and the MMMs at 50 °C at different acid concentrations.

Since all membranes are slightly hydrophilic, it is expected that the degree of swelling will increase at higher water concentrations. However, as seen in Figure 10, an opposite trend is observed. This is because acetic acid also contributes to the swelling of membranes and its effect on membrane swelling is in greater extent than that of water. Although, both water and acetic acid are polar, the swelling of membrane is affected more by the acid. This can be explained by the Hansen solubility parameter (HSP) which quantitatively describes the affinity of two or more materials with each other. Materials with similar HSP (Table A1) have high affinity for each other. The extent of the similarity in a given situation determines the extent of the interaction[55]. PEEK-WC is said to be "closer" to acetic acid than to water in the Hansen three-dimensional space given by the lower values of the solubility parameter distance, Ra (Table A2. Solubility parameter distance (Ra) of different estimation methods of Hansen solubility

parameters of PEEK-WC.). The results of the swelling experiment are consistent with the decreasing values of Ra because the polymer (and the MMMs as well) swells more as acid concentration increases. The same reasoning might also be applied for the MMMs although the HSPs and Ra values were not calculated. In general, increasing the acid concentration (lesser water concentration) increases the swelling of the MMMs.

Most membranes show negative values of swelling in water. This might be due to the residual chloroform present in the MMMs that dissolved in water during the swelling test. In the elemental analysis of the membranes, Cl is present in trace amounts. Since the MOFs were dispersed in chloroform in the preparation of the MMMs, it is also possible that chloroform molecules (kinetic diameter = 0.483 nm) occupy the pores of the MOFs and were not completely removed during oven drying.

For MZ membranes, increasing the nanofiller content from 2.5 wt% to 5 wt% increased the swelling but only up to 40% HAc. Beyond that, the swelling decreased. ZIF-8 is hydrophobic; but at higher water concentration, it is possible that water molecules occupy the pores of ZIF-8 (the size of acetic acid is bigger than the pore aperture of ZIF-8; hence it cannot enter). This is the reason why MZ-5 swells more than MZ-2.5 at higher water concentration. However, as there is less water present at higher acid concentrations, the increase in swelling of MZ membranes is highly caused by the swelling of the PEEK-WC matrix. Here, MZ-5 swells less because the volume fraction of hydrophobic component in the MMM is more.

In the case of MH membranes, increasing the nanofiller content from 2.5 wt% to 5 wt% increased the swelling in the different acid concentrations. In Figure A1, it shows that HKUST-1 has a pore aperture of 1.2 nm and a small cage of 0.5 nm. It is possible that acetic acid (0.43 nm) gets trapped in the small cages of the HKUST-1 framework. And, at higher nanofiller content, the pore volume increases, hence the swelling of MH-5 is higher than MH-2.5. Relative to neat PEEK-WC membrane, MH membranes have lower swelling degree values.

Among the MMMs, MM membranes have the highest values of swelling at higher acid concentrations (>40%). Because this MOF has both micropores and mesopores, it can accommodate higher amounts of either acetic acid/water. Compared to each other, MM-2.5 swells more because it is slightly more hydrophilic (Figure 9) than MM-5.

Because MMMs share qualities of both the matrix and the filler, it is recommended to explore the affinity of the individual MOFs, as well as the MMMs, with water and acetic acid to have a holistic analysis of not just the membrane swelling, but the other characterizations as well on how these membranes behave.

4.3. Pervaporation Experiments

As described in experimental part, PV tests were carried at 70°C (feed temperature), 10 mbar at the permeate side, and high acid concentrations (>80% HAc). Thus, the range of initial water concentration in the feed was 3-20 wt%. Because of time constraints, two feed solutions were used for the tests, i.e., one with higher water concentration (10-20 wt%) and another with lower concentration (3-7 wt%). The tests consisted in running two PV experiments (two days) for each membrane type, the first day with high feed water concentration and the second day with the low feed water concentration. The permeate side was all the time under vacuum. This procedure simulates the shutdown and startup of a PV plant in batch or continuous mode to dehydrate different acetic acid solutions. In addition, PV tests with MZ membranes were not performed due to the incompatibility of ZIF-8 with acetic acid, i.e., it is not chemically stable with acids[56].

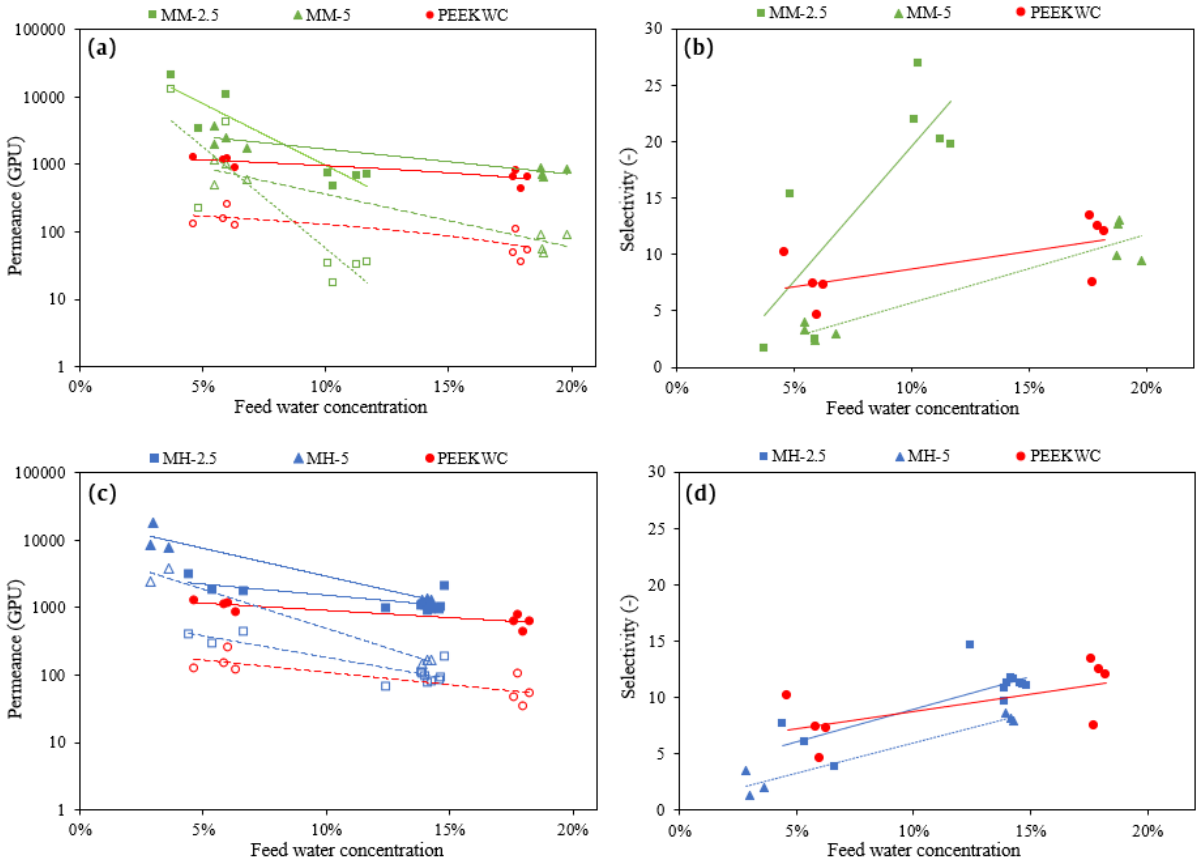

Figure 11. (a) Permeance, and (b) selectivity values of MM membranes; and (c) permeance, and (d) selectivity values of MH membranes in comparison with neat PEEK-WC membrane. Filled symbols correspond to water and unfilled symbols are for acetic acid. The Wilson model for activity coefficients calculation was used here.

Figure 11 shows the permeance and selectivity values as a function of feed water concentration for PEEK-WC membrane and different MMMs. Because water and acetic acid are polar molecules, the mixture is highly nonideal. Thus, a thermodynamic model is required

to calculate the liquid activity coefficients to calculate driving forces (partial vapor pressures) and permeances of permeating molecules[22]. Since water and acetic acid are totally miscible, the Wilson model is apt to use for the activity coefficient calculation. The permeances were also calculated using the NRTL model for comparison (Figure A4.), but there are no significant differences.

Among the five membrane samples, only two membranes (PEEK-WC and MH-2.5) gave stable permeance values (Figure 11) within this range of feed water concentration. For these two membranes, there is a good visual gap between the permeance of water and acetic acid. The water permeance of the membrane MH-2.5 (2168 GPU) at 15 wt% water in the feed is more than three times higher than that of PEEK-WC (642 GPU). At higher acid concentration (5 wt% water) in the feed, the water permeance is also high (see Table 9). The selectivity values of these two membranes are similar, hence the addition of nanoparticles (MH) enhances the permeance. However, higher content of nanoparticles seems to be inconvenient since MH-5 lost its selectivity.

Table 9. Permeance and selectivity values of the different membranes.

Membrane	%Water in feed	P_W [GPU]	P_A [GPU]	$\alpha_{W/A}$ [-]
PEEK-WC	5	1145	156	7.3
	15	642	54	12
MH-2.5	5	3176	415	7.7
	15	2168	195	11.1
MH-5	5	7876	3873	2.0
	15	1364	168	8.1
MM-2.5	5	10780	4246	2.5
	15	717	36	19.7
MM-5	5	3760	1130	3.3
	15	893	90	9.9

The swelling results are in good agreement with the results obtained from the pervaporation tests. MH-2.5 has low values of swelling at 80% HAc and it gave high values of permeance. This means that the nanofiller provided additional means of transport for water to permeate through the membrane without losing the selectivity. MM-2.5, on the other hand, swells more at 80% HAc; and thus, it has the highest water permeance as well. However, this high swelling made the membrane lose its selectivity and allow acetic acid to permeate as well.

Although the permeance and selectivity values are high for MM-2.5 at 15 wt% water in the feed, the permeance increased 15 times when the water concentration was down to 5 wt%. And at the same time, the selectivity dropped from 19.7 to 2.5. This might be due to the nanofillers being removed from the matrix, leaving holes (pores) along the membrane which

allows both components from the mixture to permeate (Figure 11 shows a sharp increase of acetic acid and water permeance when the water concentration in the feed changes from 10% to 5%). It is important to note that the permeance values are plotted in a logarithmic scale so a visual decline in the plot (e.g., MM-2.5) means a significant decline in permeance values. Compared to MH membranes, MM membranes are less selective to water.

As a general trend, as the amount of water in the feed decreases (higher acid concentrations), the membranes become less selective, especially MM membranes. The permeance of water is always higher than the permeance of acetic acid, which resulted in selectivity values between 2.0 and 19.7. PEEK-WC and MH-2.5 give the most stable membrane in acetic acid as evidenced by its good permeance without losing abruptly the selectivity. The addition of nanofiller clearly shows that the water permeance in PEEK-WC can be improved. However, the content of nanofiller must be minimized to keep the selectivity, at least for MH membranes. As seen above, higher content of nanofillers (5 wt%) leads to membranes with lower selectivity. Although, it is also possible that with other nanofillers, a different trend can be obtained.

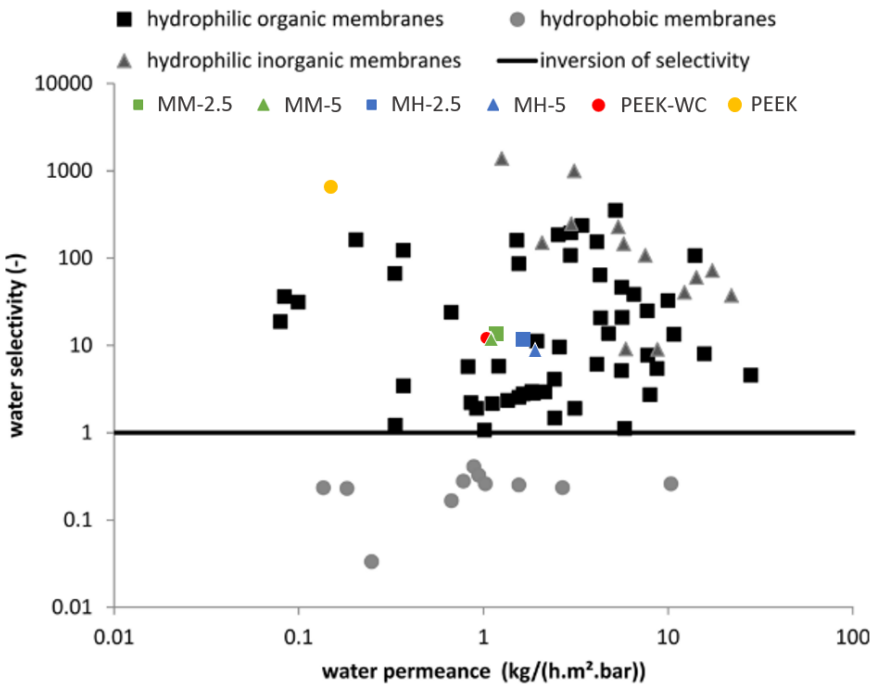

Figure 12. Water selectivity versus water permeance for different membranes whose performances have been published in the literature[22] with the membranes prepared in this work incorporated. The data for hydrophilic membranes are limited to those reports with working temperature of 30-65 °C and a feed water composition of 10-20 wt% to compare with the operating parameters done in this work.

Due to time constraints, the characterization of the membranes after the PV test was not done. Additional characterizations will provide more information to understand the performance and behavior of membranes. Moreover, the scope of this work only includes two

filler contents. It is difficult to conclude if the obtained trends are general trends for an increase or decrease of the nanofiller content.

Figure 12 shows how the membranes prepared in this work performed in comparison to the pervaporation performance of different membranes published in literature[22]. All the membranes are in the average range of selectivity and permeance values. PEEK (without the modified cardo group) has high water selectivity, almost in the range of hydrophilic inorganic membranes), but the water permeance of water is very low. Also, as mentioned above, it is very difficult to dissolve PEEK which makes the membrane preparation difficult as well. It is important to note that these are just one data point. We have seen above that it is possible to have high selectivity and high permeance at one point, and then a sharp decline in the selectivity. The selectivity values reported might be high but the water permeance might not also be stable. Thus, to have a good comparison of developed membranes, if possible, the permeances and the selectivity values should be assessed across the range of feed water concentration used to better evaluate the membrane performances.

5. Conclusion and Recommendations

Defect-free PEEK-WC membrane film with thickness of less than 10 μm was successfully prepared by varying the casting speed thickness. Three metal-organic frameworks were successfully synthesized and characterized: ZIF-8, HKUST-1, and MIL-101(Cr). Different synthesis methods were used based on their non-complexity, synthesis time, and their use of less toxic solvents. All the results of the characterization (SEM, XRD, TGA and N_2 sorption analysis) are in good agreement with those reported in literature.

The MOFs (in 2.5 and 5.0 wt%) were successfully incorporated into the PEEK-WC matrix and the films of less than 10 μm were also prepared without any defects. The nanofillers have good dispersion in the membrane. All MMMs are slightly hydrophilic in nature and show good thermal stability. Increasing the nanofiller content increased the Young's modulus of the neat polymer for MZ and MH membranes, but it decreased for MM membranes. All the MMMs have lower break strength; and except for MZ membranes, the rest of the MMMs are more brittle than the neat polymer.

In general, all membranes have higher degrees of swelling when the acid concentration is increased. Aside from MM membranes, all MMMs have lower degrees of swelling than neat PEEK-WC at higher acid concentrations with MZ-5 and MH-2.5 having the lowest swelling at 80% HAc. To explain more the effect of nanofillers on swelling, it is recommended to investigate the affinity of the individual MOFs, as well as the MMMs, with water and acetic acid; and to explore a broader range of nanofiller contents to confirm the trends obtained.

The addition of nanofillers in the PEEK-WC matrix all increased the permeance of water, but only MH-2.5 kept the neat membrane's selectivity at high acid concentration (5%). The water permeance increased almost threefold (PEEK-WC: 1142 GPU, MH-2.5: 3176 GPU) while keeping the selectivity of the neat PEEK-WC membrane. Increasing further the nanofiller content to 5 wt% (MH-5) loses the selectivity. Hence, lower nanofiller contents for MH membranes can be investigated.

This paper shows that it is possible to develop MMMs, with PEEK-WC as the matrix, which have promising performance in pervaporation for the dehydration of acetic acid. The membrane performances fall within the range of performances published in literature. However, there are still a lot of points for improvement to have a more holistic understanding of these MMMs. Here are some of the recommendations for future work:

(1) Optimize the nanofiller size. Better properties and performance might be obtained by decreasing the size of the nanofiller. Also, the smaller the nanofiller size, the thinner the membranes can be prepared.

(2) Explore broader range of nanofiller content to better evaluate the effect of nanofillers in the performance of the mixed-matrix membranes in pervaporation.

(3) Repeat pervaporation tests on all membranes to confirm the results obtained and characterize them after the test.

(4) Perform stability tests on the membranes which showed promising performance to check if they are suitable for long-term operation use.

(5) Lastly, analyze the data obtained using the different models available to predict permeability in mixed matrix membranes to have a better understanding of the mechanism of permeation of HAc and H_2O and the behavior of the membranes.

References

1. *Acetic Acid Market for VAM, Acetate Esters, Acetic Anhydride, PTA and Other Application: Global Industry Perspective, Comprehensive Analysis and Forecast, 2015 - 2021*. https://www.zionmarketresearch.com/market-analysis/acetic-acid-market (2016).

2. *Global Acetic Acid Market to Reach 11.85 Million Tons by 2026*. https://www.expertmarketresearch.com/pressrelease/global-acetic-acid-market (2020).

3. Dmitrenko, M. E. *et al.* Development and investigation of mixed-matrix PVA-fullerenol membranes for acetic acid dehydration by pervaporation. *Sep. Purif. Technol.* **187**, 285–293 (2017).

4. Jullok, N., Deforche, T., Luis, P. & Van der Bruggen, B. Sorption and diffusivity study of acetic acid and water in polymeric membranes. *Chem. Eng. Sci.* **78**, 14–20 (2012).

5. Servel, C., Favre, E. & Roizard, D. Possibilities and limitations of pervaporation for improved acetic acid dehydration by distillation at industrial scale: A critical analysis. in *Procedia Engineering* vol. 44 2065–2067 (Elsevier Ltd, 2012).

6. Dimian, A. C., Bildea, C. S. & Kiss, A. A. Acetic Acid. in *Applications in Design and Simulation of Sustainable Chemical Processes* (Elsevier, 2019). doi:10.1016/B978-0-444-63876-2.00013-9.

7. You, X., Gu, J., Peng, C., Donis, I. R. & Liu, H. Optimal design of extractive distillation for acetic acid dehydration with N-methyl acetamide. *Chem. Eng. Process.* **120**, (2017).

8. Raza, W., Wang, J., Yang, J. & Tsuru, T. Progress in pervaporation membranes for dehydration of acetic acid. *Sep. Purif. Technol.* **262**, 118338 (2021).

9. Brüschke, H. E. A. State-of-the-Art of Pervaporation Processes in the Chemical Industry. in *Membrane Technology: in the Chemical Industry, Second, Revised and Extended Edition* 151–202 (Wiley-VCH Verlag GmbH & Co. KGaA, 2006). doi:10.1002/3527608788.ch10.

10. Figoli, A., Santoro, S., Galiano, F. & Basile, A. Pervaporation membranes: Preparation, characterization, and application. in *Pervaporation, Vapour Permeation and Membrane Distillation: Principles and Applications* 19–63 (Elsevier Ltd, 2015). doi:10.1016/B978-1-78242-246-4.00002-7.

11. Vane, L. M. Review: membrane materials for the removal of water from industrial solvents by pervaporation and vapor permeation. *J. Chem. Technol. Biotechnol.* **94**, (2019).

12. Das, P. & Ray, S. K. Analysis of sorption and permeation of acetic acid-water mixtures through unfilled and filled blend membranes. *Sep. Purif. Technol.* **116**, 433–447 (2013).

13. Chaudhari, S. *et al.* In Situ Generation of Silver Nanoparticles in Poly(Vinyl Alcohol)/Poly(Acrylic Acid) Polymer Membranes in the Absence of Reducing Agent and their Effect on Pervaporation of a Water/Acetic Acid Mixture. *Bull. Korean Chem. Soc.* **37**, 1985–1991 (2016).

14. Su, Z., Chen, J. H., Sun, X., Huang, Y. & Dong, X. Amine-functionalized metal organic framework (NH2-MIL-125(Ti)) incorporated sodium alginate mixed matrix membranes for dehydration of acetic acid by pervaporation. *RSC Adv.* **5**, 99008–99017 (2015).

15. Bhat, S. D. & Aminabhavi, T. M. Pervaporation-aided dehydration and esterification of acetic acid with ethanol using 4A zeolite-filled cross-linked sodium alginate-mixed matrix membranes. *J. Appl. Polym. Sci.* **113**, 157–168 (2009).

16. Chapman, P. D., Oliveira, T., Livingston, A. G. & Li, K. Membranes for the dehydration of solvents by pervaporation. *Journal of Membrane Science* vol. 318 5–37 (2008).

17. Zhu, M. H. *et al.* Rapid preparation of acid-stable and high dehydration performance mordenite membranes. *Ind. Eng. Chem. Res.* **53**, 19168–19174 (2014).

18. Lecaros, R. L. G. *et al.* Tunable interlayer spacing of composite graphene oxide-framework membrane for acetic acid dehydration. *Carbon N. Y.* **123**, 660–667 (2017).

19. Zereshki, S. *et al.* Effect of polymer composition in PEEKWC/PVP blends on pervaporation separation of ethanol/cyclohexane mixture. *Sep. Purif. Technol.* **75**, 257–265 (2010).

20. Van Baelen, D., Van Der Bruggen, B., Van Den Dungen, K., Degreve, J. & Vandecasteele, C. Pervaporation of water-alcohol mixtures and acetic acid-water mixtures. *Chem. Eng. Sci.* **60**, 1583–1590 (2005).

21. Li, W. *et al.* Sorption and pervaporation study of methanol/dimethyl carbonate mixture with poly(etheretherketone) (PEEK-WC) membrane. *J. Memb. Sci.* **567**, 303–310 (2018).

22. Servel, C., Roizard, D., Favre, E. & Horbez, D. Improved energy efficiency of a hybrid pervaporation/distillation process for acetic acid production: Identification of target membrane performances by simulation. *Ind. Eng. Chem. Res.* **53**, 7768–7779 (2014).

23. Kulkarni, S. S., Tambe, S. M., Kittur, A. A. & Kariduraganavar, M. Y. Preparation of novel composite membranes for the pervaporation separation of water-acetic acid mixtures. *J. Memb. Sci.* **285**, 420–431 (2006).

24. Castro-Munoz, R., Iglesia, Ó. D. La, Fíla, V., Téllez, C. & Coronas, J. Pervaporation-Assisted Esterification Reactions by Means of Mixed Matrix Membranes. *Ind. Eng. Chem. Res.* **57**, 15998–16011 (2018).

25. Deng, Y.-H. *et al.* A Drying-Free, Water-Based Process for Fabricating Mixed-Matrix Membranes with Outstanding Pervaporation Performance. *Angew. Chemie* **128**, 12985–12988 (2016).

26. Esposito, E. *et al.* Glassy PEEK-WC vs. Rubbery Pebax®1657 Polymers: Effect on the Gas Transport in CuNi-MOF Based Mixed Matrix Membranes. *Appl. Sci.* **10**, 1310 (2020).

27. Cavka, J. H. *et al.* A new zirconium inorganic building brick forming metal organic frameworks with exceptional stability. *J. Am. Chem. Soc.* **130**, 13850–13851 (2008).

28. Zhu, M. H., Kumakiri, I., Tanaka, K. & Kita, H. Dehydration of acetic acid and esterification product by acid-stable ZSM-5 membrane. *Microporous Mesoporous Mater.* **181**, 47–53 (2013).

29. Yang, J. *et al.* Tuning aluminum spatial distribution in ZSM-5 membranes: A new strategy to fabricate high performance and stable zeolite membranes for dehydration of acetic acid. *Chem. Commun.* **50**, 14654–14657 (2014).

30. Jose, T., George, S. C., Mg, M. & Thomas, S. Functionalized MWCNT and PVA Nanocomposite Membranes for Dielectric and Pervaporation Applications. *J Chem Eng Process Technol* **6**, 233 (2015).

31. Clarizia, G., Algieri, C., Regina, A. & Drioli, E. Zeolite-based composite PEEK-WC membranes: Gas transport and surface properties. *Microporous Mesoporous Mater.* **115**, 67–74 (2008).

32. Adoor, S. G., Sairam, M., Manjeshwar, L. S., Raju, K. V. S. N. & Aminabhavi, T. M. Sodium montmorillonite clay loaded novel mixed matrix membranes of poly(vinyl alcohol) for pervaporation dehydration of aqueous mixtures of isopropanol and 1,4-dioxane. *J. Memb. Sci.* **285**, 182–195 (2006).

33. Huang, Y. *et al.* Pervaporation of ethanol aqueous solution by polydimethylsiloxane/polyphosphazene nanotube nanocomposite membranes. *J. Memb. Sci.* **339**, 85–92 (2009).

34. Samanta, H. S., Ray, S. K., Das, P. & Singha, N. R. Separation of acid-water mixtures by pervaporation using nanoparticle filled mixed matrix copolymer membranes. *J. Chem. Technol. Biotechnol.* **87**, (2012).

35. Jia, Z. & Wu, G. Metal-organic frameworks based mixed matrix membranes for pervaporation. *Microporous and Mesoporous Materials* vol. 235 151–159 (2016).

36. Wang, N. *et al.* Pervaporation dehydration of acetic acid using NH2-UiO-66/PEI mixed matrix membranes. *Sep. Purif. Technol.* **186**, 20–27 (2017).

37. Jullok, N. *et al.* Effect of silica nanoparticles in mixed matrix membranes for pervaporation dehydration of acetic acid aqueous solution: Plant-inspired dewatering systems. *J. Clean. Prod.* **112**, 4879–4889 (2016).

38. Zhang, Y. *et al.* All-silica DD3R zeolite membrane with hydrophilic-functionalized surface for efficient and highly-stable pervaporation dehydration of acetic acid. *J. Memb. Sci.* **581**, 236–242 (2019).

39. Gao, R. *et al.* Highly efficient polymer–MOF nanocomposite membrane for pervaporation separation of water/methanol/MTBE ternary mixture. *Chem. Eng. Res. Des.* **117**, 688–697 (2017).

40. Chen, J. H., Liu, Q. L., Xiong, Y., Zhang, Q. G. & Zhu, A. M. Composite membranes prepared from glutaraldehyde cross-linked sulfonated cardo polyetherketone and its blends for the dehydration of acetic acid by pervaporation. *J. Memb. Sci.* **325**, 184–191 (2008).

41. Zereshki, S. *et al.* Pervaporation separation of MeOH/MTBE mixtures with modified PEEK membrane: Effect of operating conditions. *J. Memb. Sci.* **371**, 1–9 (2011).

42. Xin, Q. *et al.* Mixed matrix membranes composed of sulfonated poly(ether ether ketone) and a sulfonated metal-organic framework for gas separation. *J. Memb. Sci.* **488**, 67–78 (2015).

43. Kida, K., Okita, M., Fujita, K., Tanaka, S. & Miyake, Y. Formation of high crystalline ZIF-8 in an aqueous solution. *CrystEngComm* **15**, 1794–1801 (2013).

44. Karimi, A., Khataee, A., Vatanpour, V. & Safarpour, M. High-flux PVDF mixed matrix membranes embedded with size-controlled ZIF-8 nanoparticles. *Sep. Purif. Technol.* **229**, 115838 (2019).

45. Pan, Y., Liu, Y., Zeng, G., Zhao, L. & Lai, Z. Rapid synthesis of zeolitic imidazolate framework-8 (ZIF-8) nanocrystals in an aqueous system. *Chem. Commun.* **47**, 2071–2073 (2011).

46. de la Iglesia, Ó. *et al.* Metal-organic framework MIL-101(Cr) based mixed matrix membranes for esterification of ethanol and acetic acid in a membrane reactor. *Renew. Energy* **88**, 12–19 (2016).

47. Wee, L. H., Lohe, M. R., Janssens, N., Kaskel, S. & Martens, J. A. Fine tuning of the metal-organic framework Cu 3(BTC) 2 HKUST-1 crystal size in the 100 nm to 5 micron range. *J. Mater. Chem.* **22**, 13742–13746 (2012).

48. Huo, J., Brightwell, M., El Hankari, S., Garai, A. & Bradshaw, D. A versatile, industrially relevant, aqueous room temperature synthesis of HKUST-1 with high space-time yield. *J. Mater. Chem. A* **1**, (2013).

49. Khan, N. A., Kang, I. J., Seok, H. Y. & Jhung, S. H. Facile synthesis of nano-sized metal-organic frameworks, chromium-benzenedicarboxylate, MIL-101. *Chem. Eng. J.* **166**, 1152–1157 (2011).

50. Shi, Z., Yu, Y., Fu, C., Wang, L. & Li, X. Water-based synthesis of zeolitic imidazolate framework-8 for CO2 capture. *RSC Adv.* **7**, 29227–29232 (2017).

51. Majano, G. & Pérez-Ramírez, J. Room temperature synthesis and size control of HKUST-1. *Helv. Chim. Acta* **95**, 2278–2286 (2012).

52. Khan, N. A., Jun, J. W. & Jhung, S. H. Effect of Water Concentration and Acidity on the Synthesis of Porous Chromium Benzenedicarboxylates. *Eur. J. Inorg. Chem.* **2010**, 1043–1048 (2010).

53. Férey, G. *et al.* A Chromium Terephthalate-Based Solid with Unusually Large Pore Volumes and Surface Area. *Science (80-.).* **309**, 2040–2042 (2005).

54. Decoste, J. B., Denny, M. S., Peterson, G. W., Mahle, J. J. & Cohen, S. M. Enhanced aging properties of HKUST-1 in hydrophobic mixed-matrix membranes for ammonia adsorption †. (2016) doi:10.1039/c5sc04368a.

55. Hansen, C. M. Hansen Solubility Parameters : A User's Handbook, Second Edition. *Hansen Solubility Parameters A Users Handbook, Second Ed.* 113–123 (2007) doi:10.1201/9781420006834.

56. Gao, S. *et al.* Improving the Acidic Stability of Zeolitic Imidazolate Frameworks by Biofunctional Molecules. *Chem* **5**, 1597–1608 (2019).

57. Zhao, T. *et al.* Facile synthesis of nano-sized MIL-101(Cr) with the addition of acetic acid. *Inorganica Chim. Acta* **471**, 440–445 (2018).

58. Railey, P., Song, Y., Liu, T. & Li, Y. Metal organic frameworks with immobilized nanoparticles: Synthesis and applications in photocatalytic hydrogen generation and energy storage. *Mater. Res. Bull.* **96**, 385–394 (2017).

ANNEX

I. Figures

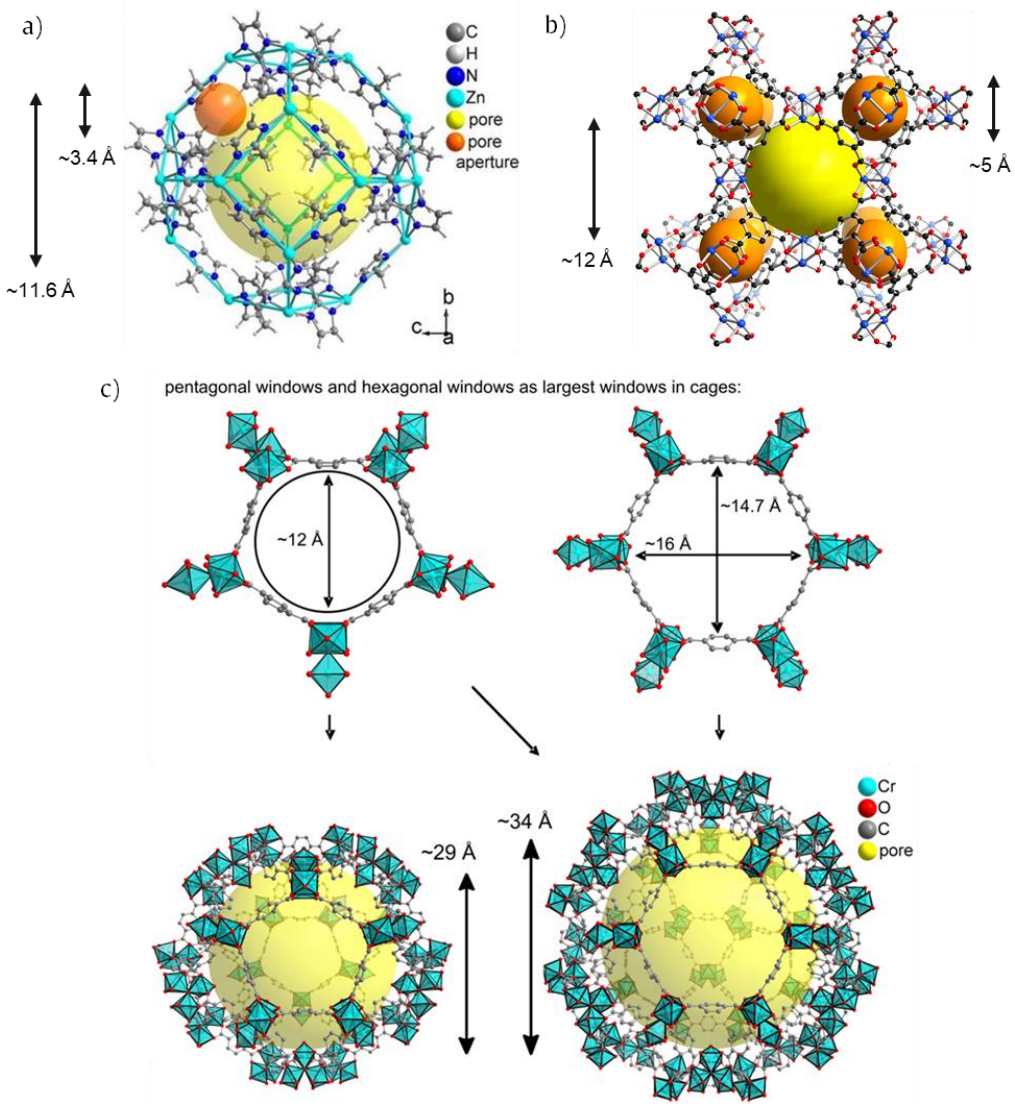

Figure A1. Structures of the different MOFs with the dimensions of their cages and pore apertures: (a) ZIF-8[57], (b) HKUST-1, and (c) MIL-101(Cr)[58].

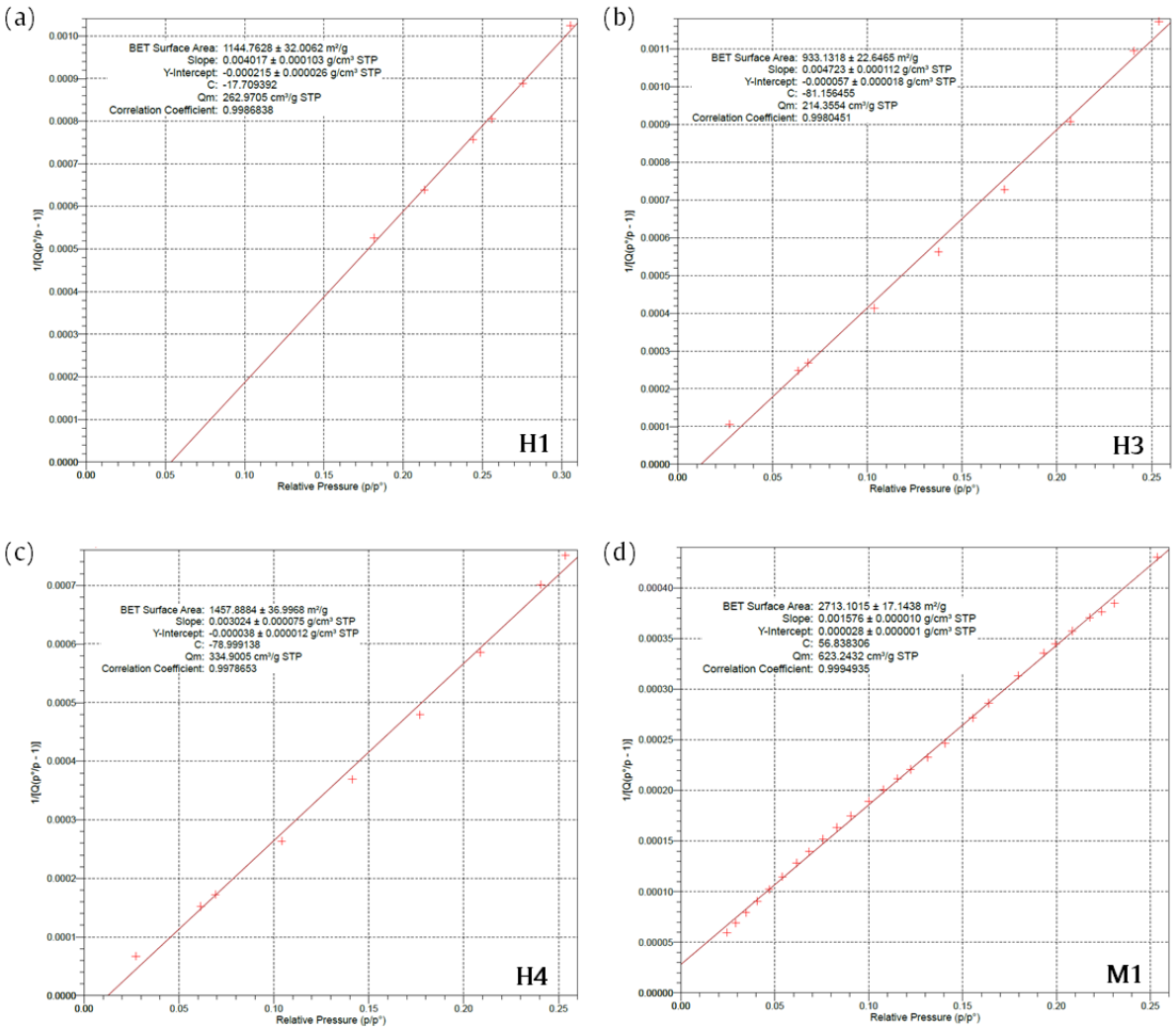

Figure A2. BET calculations for each sample, including correlation coefficient, Qm, C constant, BET curve slope and y-intercept.

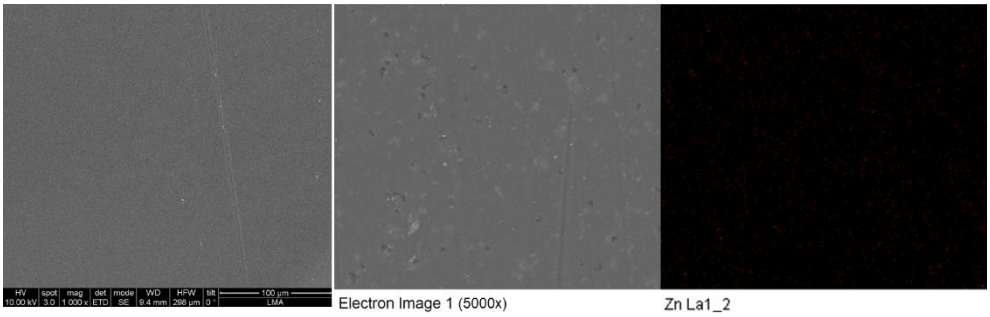

MZ-2.5

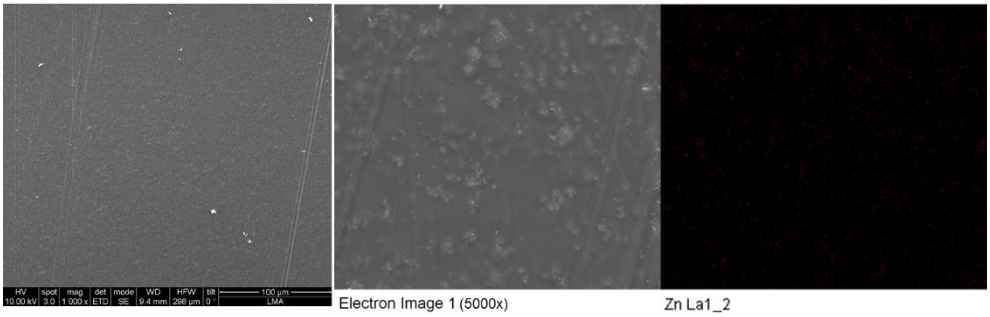

MZ-5

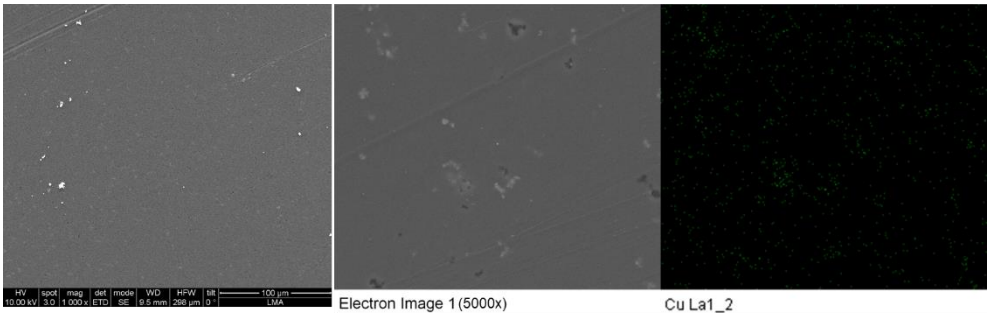

MH-2.5

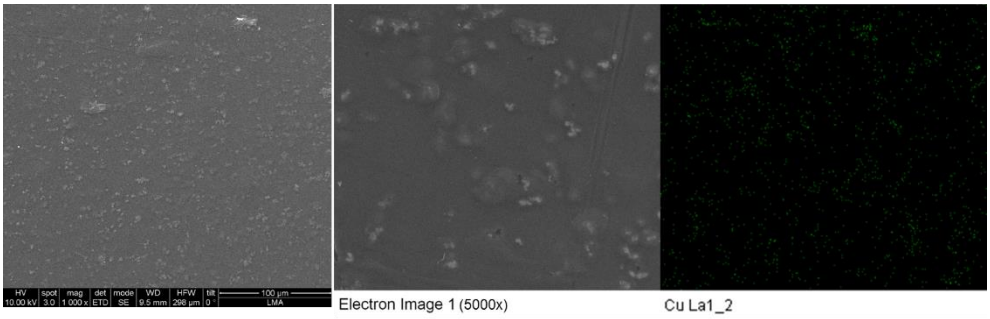

MH-5

Figure A3. Elemental analysis of the MZ and MH membranes according to their metal center. MM membranes were not analyzed due to lack of time.

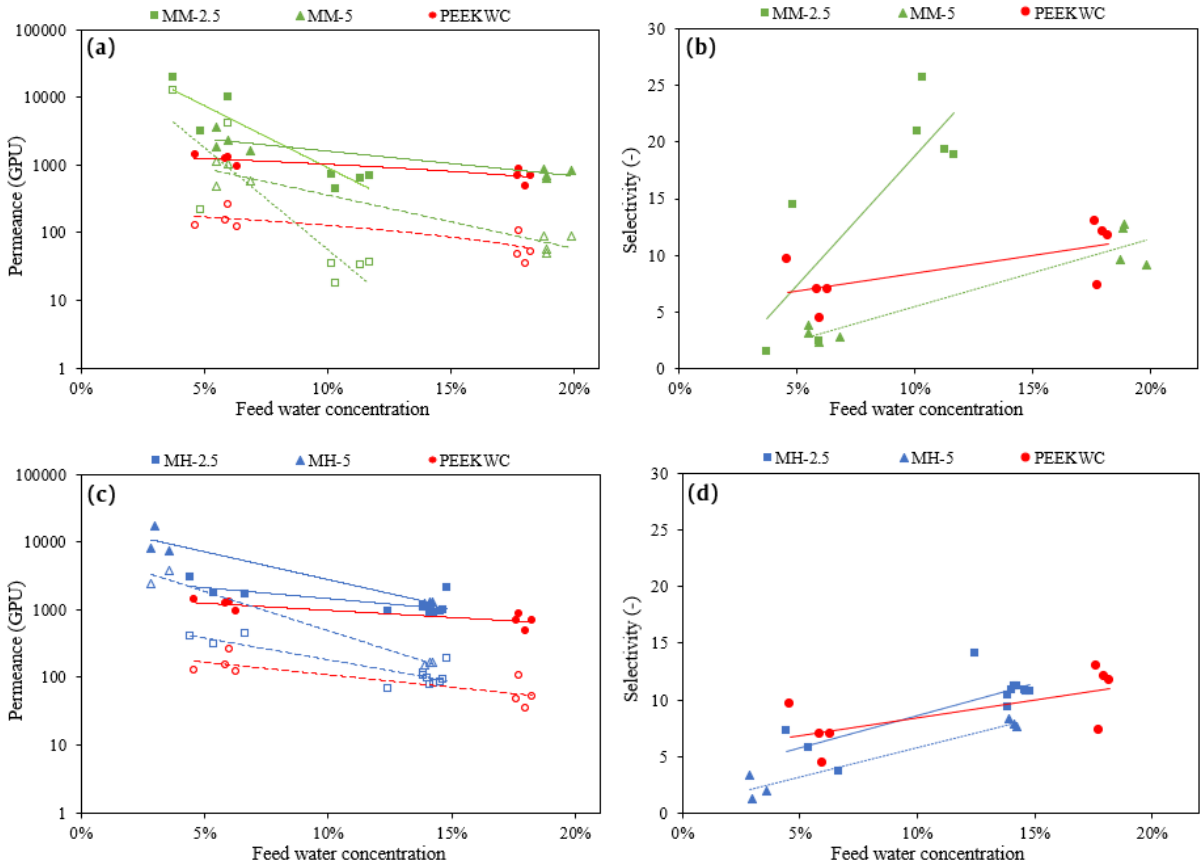

Figure A4. (a) Permeance, and (b) selectivity values of MM membranes; and (c) permeance, and (d) selectivity values of MH membranes in comparison with neat PEEK-WC membrane. Filled symbols correspond to water and unfilled symbols are for acetic acid. The NRTL model for activity coefficients calculation was used here.

2. Tables

Table A1. Hansen solubility parameters of pure water, acetic acid, PEEK-WC using several estimation methods, and the different HAc/H_2O mixtures.

Material	Method	δ_D	δ_P	δ_H	δ_t
Water		18.1	17.1	16.9	30.1
Acetic Acid		14.5	8	13.5	21.4
PEEK-WC[21]	Yamamoto	19.2	8.3	3.9	21.3
	Stefanis-Panayiotou	25.5	-8	5.6	27.3
	Van Krevelen	18.9	2.8	6.2	20.1
	Hoy	16.5	11	14.6	24.6
Mixture					
0% HAc		18.1	17.1	16.9	30.1
20% HAc		17.4	15.3	16.2	28.3
40% HAc		16.7	13.5	15.5	26.6
60% HAc		15.9	11.6	14.9	24.9
80% HAc		15.2	9.8	14.2	23.1
100% HAc		14.5	8.0	13.5	21.4

Table A2. Solubility parameter distance (Ra) of different estimation methods of Hansen solubility parameters of PEEK-WC.

Material	Yamamoto	Stefanis-Panayiotou	Van Krevelen	Hoy
Water	15.9	31.3	17.9	7.3
Acetic Acid	13.4	28.3	12.6	5.1
Mixture				
0% HAc	15.9	31.3	17.9	7.3
20% HAc	14.6	30.3	16.3	4.9
40% HAc	13.7	29.5	14.9	2.7
60% HAc	13.2	28.9	13.7	1.3
80% HAc	13.1	28.5	12.9	2.8
100% HAc	13.4	28.3	12.6	5.1

Table A3. Data values of normalized fluxes, selectivities and permeances using WILSON and NRTL model.

Membrane	$\%H_2O^F$	J_{total} (μm·kg/m²/h)	J_W (μm·kg/m²/h)	J_A (μm·kg/m²/h)	α_{WILSON} (-)	α_{NRTL} (-)	$P_{W,WILSON}$ (GPU)	$P_{W,NRTL}$ (GPU)	$P_{A,WILSON}$ (GPU)	$P_{A,NRTL}$ (GPU)
MM-2.5	11.7%	3.37	2.86	0.51	19.7	18.9	717	686	36	36
	10.1%	3.26	2.76	0.50	22.0	21.0	754	720	34	34
	11.3%	3.09	2.62	0.47	20.2	19.3	671	642	33	33
	10.3%	2.00	1.75	0.26	26.9	25.8	477	455	18	18
	4.8%	10.79	7.13	3.66	15.3	14.5	3402	3229	222	222
	5.9%	94.19	28.05	66.13	2.5	2.4	10780	10267	4246	4245
	3.7%	243.62	37.42	206.20	1.6	1.6	20773	19767	12667	12667
MM-5	19.8%	8.95	7.28	1.67	9.4	9.2	866	840	92	91
	18.7%	8.97	7.30	1.67	9.9	9.6	893	864	90	90
	18.8%	6.91	5.86	1.05	12.7	12.4	720	697	57	56
	18.9%	6.22	5.31	0.92	13.1	12.8	651	630	50	49
	6.8%	21.58	7.72	13.86	3.0	2.8	1744	1662	590	590
	5.5%	19.49	7.38	12.12	4.0	3.8	1988	1891	496	496
	5.5%	41.76	14.07	27.70	3.3	3.1	3761	3579	1138	1138
	5.9%	34.46	9.89	24.57	2.4	2.3	2467	2350	1026	1026
MH-2.5	14.6%	2.92	2.34	0.58	11.3	10.9	978	940	86	86
	14.0%	3.29	2.61	0.68	11.2	10.8	1116	1072	99	99
	13.9%	3.46	2.72	0.74	10.8	10.4	1170	1124	108	108
	13.9%	3.40	2.61	0.79	9.7	9.4	1116	1072	115	115
	14.6%	3.14	2.51	0.63	11.2	10.8	1043	1003	93	93
	14.3%	2.81	2.26	0.56	11.7	11.3	951	915	82	81
	14.8%	6.57	5.26	1.32	11.1	10.7	2168	2086	195	194
	12.4%	2.69	2.20	0.49	14.7	14.1	1010	968	69	68
	14.1%	2.65	2.12	0.53	11.7	11.3	904	869	77	77
	6.6%	6.15	2.56	3.59	3.9	3.7	1765	1681	451	451
	5.3%	4.79	2.25	2.54	6.1	5.8	1857	1766	306	306
	4.4%	6.80	3.27	3.53	7.7	7.3	3176	3017	415	415
MH-5	14.1%	4.47	3.30	1.17	8.1	7.8	1364	1311	168	168
	14.2%	4.45	3.27	1.18	7.9	7.6	1347	1295	170	170
	13.9%	4.17	3.12	1.06	8.6	8.3	1302	1251	151	151
	2.8%	27.56	6.31	21.26	3.6	3.4	8606	8175	2405	2406
	3.6%	40.10	7.16	32.94	2.0	1.9	7876	7489	3873	3873
	3.0%	132.39	14.49	117.89	1.4	1.3	18356	17469	13450	13451
PEEK-WC	17.7%	3.27	2.49	0.78	7.5	7.3	810	880	108	107
	18.2%	2.38	1.99	0.39	12.0	11.7	642	698	54	53
	17.6%	2.30	1.95	0.35	13.3	13.0	639	694	48	48
	18.0%	1.62	1.37	0.26	12.4	12.1	443	481	36	35
	6.3%	2.56	1.41	1.15	7.2	6.9	891	959	123	124
	4.6%	2.83	1.58	1.25	10.1	9.6	1293	1392	128	128
	5.8%	3.18	1.71	1.47	7.3	7.0	1145	1224	156	156
	6.0%	4.27	1.85	2.42	4.6	4.4	1198	1282	259	259